CHAPTER N: COMPARTMENTAL MODELING IN THE ANALYSIS OF BIOLOGICAL SYSTEMS.

James B Bassingthwaighte, Erik Butterworth, Bartholomew Jardine, and Gary M Raymond. Department of Bioengineering, University of Washington, Seattle WA 98195-5061

Summary:

Compartmental models are composed of sets of interconnected mixing chambers or stirred tanks. Each component of the system is considered to be homogeneous, instantly mixed, with uniform concentration. The state variables are concentrations or molar amounts of chemical species. Chemical reactions, transmembrane transport and binding processes, determined in reality by electrochemical driving forces and constrained by thermodynamic laws, are generally treated using first order rate equations. This fundamental simplicity makes them easy to compute since ordinary differential equations (ODEs) are readily solved numerically and often analytically. While compartmental systems have a reputation for being merely descriptive they can be developed to levels providing realistic mechanistic features through refining the kinetics. Generally, one is considering multi-compartmental systems for realistic modeling. Compartments can be used as "black" box operators without explicit internal structure, but in pharmacokinetics compartments are considered as homogeneous pools of particular solutes, with inputs and outputs defined as flows or solute fluxes, and transformations expressed as rate equations.

Descriptive models providing no explanation of mechanism are nevertheless useful in modeling of many systems. In pharmacokinetics (PK), compartmental models are in widespread use for describing the concentration-time curves of a drug concentrations following administration. This gives a description of how long it remains available in the body, and is a guide to defining dosage regimens, method of delivery, and expectations for its effects. Pharmacodynamics (PD) requires more depth since it focuses on the physiological response to the drug or toxin, and therefore stimulates a demand to understand how the drug works on the biological system; having to understand drug response mechanisms then folds back on the delivery mechanism (the PK part) since PK and PD are going on simultaneously (PKPD).

Many systems have been developed over the years to aid in modeling PKPD systems. Almost all have solved only ODEs though allowing considerable conceptual complexity in the descriptions of chemical transformations, methods of solving the equations, displaying results, and analyzing systems behavior. Systems for compartmental analysis include SAAM (Simulation and Applied Mathematics), CoPasi (enzymatic reactions), Berkeley Madonna (physiological systems), XPPaut (dynamical system behavioral analysis) and a good many others. JSim, a system allowing the use of both ODEs and PDEs (partial differential equations that describe spatial distributions), is used here. It is an open source system, meaning that it is available for free and can be modified by users. It offers a set of features unique in breadth of capability that make model verification surer and easier, and produces models that can be shared on all standard computer platforms.

Key Words: physiological and pharmacologic modeling, PKPD, pharmacokinetics – pharmacodynamics, compartmental systems, systems biology, Physiome, JSim, CellML, SBML. Reproducible research, unit checking, verification, validation, ordinary and partial differential equations, optimization, confidence limits.

1. Introduction

1.1 Overview of the topic:

Compartmental analysis implies the use of linear first order differential operators as analogs for describing the kinetics of drug distribution and elimination from the body. Concentrations are measured in accessible fluids, usually the plasma, and the concentration-time curve is used to provide a measure of how long the drug concentration remains at a therapeutic level. This is the basis of *pharmacokinetics* (*PK*). The influences on efficacy and utility are considered by the term ADME, administration, distribution, metabolism and elimination. Drugs are given in chemically significant amounts, and are involved in biochemical reactions, binding to proteins, receptors or transporters in concentration-dependent fashion, are metabolized in enzymatic reactions: the effect on the biological system is the *pharmacodynamics (PD)*. Precise mathematical statements about the kinetics and the body's responses comprise the combination *pharmacokinetics-pharmacodynamics* (*PKPD*).

Compartmental analysis had its historical start with the use of tracers. Tracer-labeled compounds were used in order to determine kinetics when the drug concentrations were too low to be measured chemically. Radioactive tracers were given in such low concentrations relative to those of native non-tracer mother substances that the kinetics were in fact linear. Consider a reaction rate, k(C), that is dependent upon the concentration of the mother substance of concentration C(t):

$$\text{Flux of Mother Substance} = k(C) \times C(t). \qquad [1]$$

When tracer of concentration C' is added to the system, then:

$$\text{Total Flux, Mother and Tracer} = k(C + C') \times [C(t) + C'(t)]. \qquad [2]$$

When C' << C, then the rate constant is determined solely by C, as $k(C+C') \approx k(C)$, and the rate constant is independent of the tracer concentration:

$$\text{Tracer Flux of } C'(t) = k(C)*C'(t), \qquad [3]$$

where the flux is first order in C' when the background non-tracer mother substance concentration is constant. When only the tracer is changing concentration, the k(C) is constant and the system is first order and linear. In general then, one can look upon *tracers* in compartmental systems as being linear, first order systems, though nowadays they can go far beyond that. The originators and later proponents of compartmental analysis (Berman 1963; Jacquez 1973, 1996; Cobelli, Foster and Toffolo 2000) used this simplification, but were always aware of the greater possibilities of allowing non-linear coefficients. Berman's classic 1963 article provides much more than solutions to ODEs for he outlines an important philosophic approach to modeling in general. Jacquez' books and many articles, and the book by Cobelli,

Foster and Toffolo (2000), give detailed mathematical approaches and explicit applications. The desire to use linear kinetics was not so much to avoid solving nonlinear system as it was to use linear algebra to solve the differential equations. A system of linear differential equations can be solved by matrix inversion and can provide the much desired analytical solutions. As we shall see below, analytical solutions are still desired, for they serve as verification that the numerical solutions produced by modern simulation systems are correct in specific reduced cases, and thereby imply that the non-linear system solutions in that neighborhood of parameter space are also correct. But, because most biological phenomena are non-linear, such that the rate coefficients vary with the concentrations of one or usually more solutes, and temperature, and pH, we have to acknowledge right at the start that using linear compartmental systems analysis is an approximation.

Compartmental analysis was mostly descriptive, not mechanistic. It was "Black Box", not attempting to define enzymatic reactions mechanistically, but to describe the time course, "White Box" modeling is where the innards of the operational analysis attempt to describe mechanism, not just the kinetics of a relationship. Nevertheless, the descriptive level was a success; in FDA reviews quantitative descriptions are valuable, for they distinguish groups of responses and allow categorization even when they can't provide a physiological interpretation. The plasma concentration-time data are very useful in choosing methods of administration and in defining dosage regiments.
Modern molecular biology and emerging integrative multi-scale modeling analysis likewise are changing the game. Personalized medicine is pointedly mechanistic, with cell and molecular physiology dominating in the strategies of ADME (Administration, Distribution, Metabolism and Excretion). Fortunately the huge increase in the rates of acquisition of data, causing a demand for detailed, informative but complex simulation analysis has been more than compensated for by the increases in computational speed and in improved software facilitating modeling analysis. Most importantly, software sharing is now relatively easy, and of much increased importance since comprehensive models may take years in development. Now, highly non-linear complex systems, spatially distributed or lumped, are handled with faster computation, and can include kinetics and detailed physiological pharmacodynamics (the PD of PKPD), which is the systematic analysis of the body's responses to the drug or toxin. Given the relevance of physiological transport processes (diffusion, flow, transmembrane exchange, binding) in both administration and distribution, a relatively new term, PBPK, physiologically-based pharmacokinetics has arisen to recognize the importance of incorporating anatomy and physiology into PK.

Drugs are toxins. It's only a matter of dosage. The struggle to distinguish acceptable toxicity from unacceptable toxicity is the central conflict, not just for cancer therapy but also in defining drug usage in general. Aspirin, ibuprofen, oxycodone, sugar, water, all create problems when in excess. Distinguishing "Therapeutic Dose" from "Toxic Dose" depends on the drug and on the particulars of the patient (size, age, body fat level, other drugs, physiological state and past history, genetic heritage). Many substances in our environment augment the difficulties, adding other sources of specific or general toxicity.

Drugs and toxins have many common features; for example the lipid solubility that allows easy permeation of cell membranes, so desirable in drugs, is the source of the problems with inhaled toxicants. While the body has evolved a rather general system for dealing with foreign toxicants, the P450 system in the liver that handles hundreds of different chemicals, it is also good at degrading and excreting drugs as well. As a corollary, hepatotoxicity can be a problem with drugs. Likewise, renal damage can be a risk from those drugs excreted in the urine, like ibuprofen.

Computer modeling includes all phases of ADME. The method of Administration by swallowing a pill is the commonest but isn't as fast as intravenous (i.v.) injection. Intravenous is the method with the best defined administrative kinetics, followed by intramuscular (i.m.). There are a host of other local injection types, slow release subdermally, suppositories, inhalation, sublingual absorbance, etc, all of which have different rates of drug delivery into the circulation and to the target. Since the exposure of the target to the drug is most often measured in terms of the AUC (Area Under the Curve of the drug's plasma concentration versus time) the differences amongst methods of delivery are important. The AUC is influenced by dilution in the circulation (part of Distribution), degradation by hydrolysis or metabolism (the M of ADME) and excretion (the E of ADME), so a pharmacokinetic model must include all of these. See earlier Chapters on Fundamentals of ADME and on Absorption.

Closer to the target, an enzyme, receptor, channel, transporter, or transcription regulator, much depends on physicochemical attributes of the drug or toxin. Does it bind to plasma proteins? What is the affinity of the target proteins compared to that of other competing proteins, or DNA or membrane bound proteins? What are the on- and off-rates of any competing binding sites? What is the drug's tissue/blood partition coefficient or its solubility in body fat? One of the standard ways of getting clues on the fate of the drug is to do whole body distribution studies on rats to see where it is deposited at a succession of points in time. The distribution sites of positron-labeled drug may be shown with high resolution in reconstructed 3D imaging using MicroPET (Positron Emission Tomography) systems. Such observations give data on Distribution and Excretion and sometimes Metabolism. Since the retention times in specific tissue location influence, and may dominate, the AUC (area under the curve), this information is crucial to optimizing effect on the target while minimizing toxic side effects. Modeling analysis then ideally provides specific information on all of these aspects of the kinetics, and further provides the information essential to a critical understanding of the pharmacodynamics. A by-product of a good understanding of the PK is that it allows one to consider using combined drug therapy wherein a second drug is used in advance to protect a sensitive binding site by binding to it harmlessly and preventing the toxicant drug from binding. Variants on this theme might be combining therapy with a drug preventing the activation of a receptor whose binding site accepts the drug of interest.

1.2. Model Types, Topologies, and Equation Types

A. In terms of input and output characteristics we may classify compartmental systems as closed or open:

1. **Closed system**: No sinks or source, literally, all *fluxes* between inside and outside are zero, and *external driving forces* are all zero;
2. **Open system**: There are external sinks or/and sources for some of the constituents in some of the compartments or cells. (Sinks are defined as operations via which a substance vanishes from the system; sources are operations generating a substance.)

B. In terms of interconnections amongst compartments or cells, the topology of the network is useful in defining mathematical or analytical approaches:

1. **Catenary system**: Two or more compartments arranged in series.
2. **Cyclic system**: Three or more in series, with the last connected to the first allowing a circulating flux.
3. **Mammillary**: Two or more peripheral compartments connected to a central compartment and having no cyclic components, e.g. a blood compartment connected to each organ in the body.

Equating the circulatory system, for example, to a mammillary compartmental system raises questions. "How can this be a rational description? Total circulatory mixing in humans requires many minutes. Is the rate of solute escape from blood so slow that mixing throughout the whole circulation is fast in comparison to the rate of exchange with in the organs? Solute-binding to plasma proteins might so retard escape from the blood that the approximation is adequate. Alternatively, consider the mouse, where the circulatory mixing time is a few seconds, but permeabilities are similar to those in humans, so equilibration in tissues is slow compared to circulation times; here the idea that the system is mammillary is more reasonable. The basic compartmental premises, instantaneous mixing throughout the compartment and therefore uniform internal compartmental concentrations, are almost never truly valid; being alert to this implies the next step: evaluating the error due to failure to fulfill the requirements.

In terms of types of equations, models may be expressed in many forms, but physiological models set up for solving by numerical methods are mainly in the form of ODEs, DAEs (Differential-Algebraic Equations), and PDEs. First order ODEs are central to compartmental modeling, and may be linear and non-linear, for example a Michaelis-Menten equation. A set of first order equations set up with a single variable to the left of each equal sign is said to be in state variable form. See the Background Chapters on Linear Algebra and ODEs. ODEs and DAEs may be mixed together in a model, where the DAEs define variables used in the ODEs, either implicitly or explicitly. Seeking solutions sometimes requires prior analysis, but solvers like JSim and Matlab can handle many implicit forms. PDEs are becoming more common in PKPD problems now that computation is fast. Especially recently it is being recognized that there are usually concentration gradients along the lengths of capillaries for consumed substrates and for drugs during the uptake phase; the existence of gradients violates the compartmental assumption of uniform concentration (Zierler, 1981; Anderson and Bassingthwaighte 2007) and causes errors in the estimation of permeabilities and conductance parameters of all sorts. One-dimensional PDEs usually suffice for capillary-tissue exchange since in well-perfused organs the radial distances between blood and cells are so short that radial diffusional retardation is negligible compared to membrane permeation across endothelial cells or parenchymal cell membranes.

1.3 Distribution from the site of administration

Distribution, the D of ADME, is by convection, diffusion, and permeation, and must precede the drug's therapeutic and degradative reactions at target sites or metabolic sites. Distribution includes the reversible transfer of a drug between one compartment and another. Some factors affecting drug distribution include regional blood flow rates, volumes of interstitial and cellular spaces, molecular size, polarity and binding to serum proteins or other non-target sites, forming complexes. In using the Area Under the Curve of plasma concentration versus time, one should keep in mind that plasma protein-bound drug is having no effect at the targeted site. Administration and Distribution are best treated together as it is the combination of processes that govern the effective concentration reaching the target.

Whatever the administration method (delivery on nanoparticles, laser-induced controlled release, ultrasound enhancement of intradermal diffusion, pill decomposition rates, location in gut, etc), the next phases of Distribution are physiological processes (convection, permeation, diffusion, transport across membranes or intracellular microtubular transport) are fairly well understood but not necessarily characterized for the particular drug. Heterogeneities in regional flows, capillary densities, tissue composition may have to be accounted for. These precede the reaction, binding, inhibition, or receptor-mediated responses that compose the desired patho-physiological responses. Metabolic reactions, sequestration, uptake and excretion by epithelial cells (liver, kidney, saliva, skin, etc), as by the liver's P450 system, or other reactions which inactivate (glucuronidation, glycosylation) are all a part of the ADME model and have to be considered in any PK modeling. For compounds which are degraded, the effects of the metabolic products have to be assessed for long-term effects. Compounds excreted by the liver or kidney become concentrated, even 100-fold, in the process of elimination in urine or bile, and if the drug is not conjugated or inactivated in some way there may be damage to the excretory organ, compromising the organ function and changing the pharmacokinetics after prolonged usage, and raising the AUC following each administration. Both renal glomerular filtration and tubular secretion and hepatic biliary excretion create high concentrations of the drug or metabolites.

At the level of the target, **Quantitative structure-activity relationship (QSAR)** (sometimes **QSPR**: quantitative structure-property relationship) comes into play. This is the process by which chemical structure is quantitatively correlated with biological or chemical reactivity. Biological activity can be expressed quantitatively as in the concentration of a substance required to give a certain biological response, but in the context of quantitative PK analysis, one would prefer that the PD (pharmacodynamics or biological response) be also be expressed in mechanistic terms. Additionally, when physicochemical properties or structures are expressed in numbers, one can formulate mathematical relationships, or quantitative structure-activity relationships, a model. The mathematical model may also predict the biological response to related chemical compounds. But it is the concentration of the bound agent complexed to the target site that determines the level and duration of the response.

There are a good many useful measures in considering the PK of ADME. These include, in addition to area under the curve (AUC, exposure), Cmax (maximum concentration) , Tmax (Time to Cmax), half life, clearance route and rate, volume of distribution, bioavailability in unbound form. In the steady state of long term administration one assesses the plasma

concentrations, total accumulation, linear or nonlinear PK, time-dependent changes in kinetics, and metabolites, their identity and their PK. It is the combination of PK and PD that allows knowledgeable optimization of dosage regimens. A well-developed PKPD model will account for most of these considerations and thereby be predictive and advisory to the therapist. A clear description of the kinetics allows the planning of efficient dosage regimens.

2. Software for systems description, simulation and data analysis

2A. Common software and methods used in the field

Pharmacokinetics models have been written in virtually every computer language that exists, and it is a field that has stimulated the development of a large set of relatively specialized simulation systems. A partial list of simulation software for compartmental analysis goes back half a century:

SAAM (Simulation and Applied Mathematics) was the first, developed by Mones Berman at NIH for analyzing tracer kinetics; http://depts.washington.edu/saam2/) It exists still as SAAMII.

SIMCON, a general simulation control system (Knopp, 1970), now evolved into JSim, was used to solve FORTRAN-based models of all sorts.

XPPAUT, from Bard Ermentrout (http://www.math.pitt.edu/~bard/xpp/xpp.html) . XPPAUT is particularly good for bifurcation analysis of dynamical systems.

Gepasi, now CoPasi, from Fernando Mendez, http://www.softpedia.com/progDownload/Gepasi-Download-167140.html; http://www.copasi.org/tiki-view_articles.php) CoPasi is especially good for enzymatic reactions and biochemical systems, allowing a menu of choices for reaction types.

Modelica, http://www.openmodelica.org/, is excellent to linking operators and presenting the forms of model networks. (http://www.ida.liu.se/labs/pelab/modelica/OpenSourceModelicaConsortium.html).

Jarnac is designed for symbolic or diagrammatic entry for biochemical and gene regulatory reactions. (from Herbert Sauro (1991, 2001, http://www.sys-bio.org/software/jarnac.htm)

JSim : developed from SIMCON and XSim (for X-windows linux systems, http://www.physiome.org/software/xsim/), into JSim (Raymond 2003; http://www.physiome.org/jsim/). JSim was developed by Erik Butterworth; it provides automated unit balance checking and unit conversion, thus avoiding errors due to inconsistency in the units used in the code.

Non-MEM, non-linear mixed effects modeling, is a commercial; software package providing the capability to use a wide variety of pharmacokinetic models. It is particularly designed for the analysis of sparse data sets using combinations of single patient and population data.

BioSPICE (derived from SPICE, for biology: http://sourceforge.net/projects/biospice) is designed for molecular biology. See also http://jigcell.cs.vt.edu/software.php for JigCell, based on BioSpice.

COR (Cellular Open Resource) is for a Windows environment: http://cor.physiol.ox.ac.uk/

for cellular level physiological systems. PCEnv for physiological systems is being developed from it.

Stella (http://www.iseesystems.com, a commercial system) for networks of operators such as in compartmental systems.

StochSim (http://www.ebi.ac.uk/~lenov/stochsim.html) is written explicitly for the treatment of molecular interaction when there are few molecules and interactions occur stochastically.

These simulation systems have one purpose in common: to make the programming of models simpler and to facilitate the analysis of experimental data in terms of the parameterized descriptions of the kinetics. They vary considerably with respect to their representation of physical/chemical mechanisms. Such modeling and analysis systems do not displace FORTRAN, C, C++, Java as mainstream languages, but rather they replace the front-end entry to formulate the models and interface them to data sets. None of these have the general capabilities of Matlab or Mathematica, nor do they attempt algorithmic manipulation as in Maple, but are more directly tuned to the user's needs, as will be described.

2B. A preferred simulation system, JSim

JSim is perhaps the most general of these simulation analysis systems, designed for the analysis of experimental data. It is built around a "project file, .proj", that may hold many data sets, several different models and the results of multiple analyses. JSim handles not only the ODEs (ordinary differential equations) around which traditional compartmental modeling is built, but also DAEs (differential algebraic equations), implicit functions, PDEs (partial differential equations) and stochastic equations. JSim, uniquely, and from its beginning in 1999, uses unit balance checking and automated unit conversion. (Unit balance checking assures that the units of the expressions on the left of the equal sign are the same as those on the right. Automated unit conversion means that when time is expressed in minutes a velocity expressed in cm/sec will be converted to cm/min by multiplying cm/sec by 60 sec/min.) This pair of features is a great boon in programming since in the first phase of compilation it is automating the first stage of *verification* of the model's mathematical implementation, by making sure that every equation has unitary balance. The second phase of compilation parses the details of the equations, and sequences them for efficient computation. The run-time code is compiled into Java, which now runs almost as fast as FORTRAN and C. (On a cardiovascular -respiratory system model JSim ran exactly 300 times faster than a Matlab-Simulink version of the identical model.) JSim's advantages over the ODE-based systems listed above are:

- (1) runs on Linux, Macintosh, and Windows;
- (2) is free and downloadable from www.physiome.org. On the Macintosh it takes about 30 seconds to download and install, and another 10 seconds to bring up a model;
- (3) is the only one that solves partial differential equations, PDEs, and offers an assortment of solvers for both PDEs (3 available now) and ODEs (8 available),
- (4) imports and runs both SBML and CellML archival forms;
- (5) provides sensitivity analysis of two types, relative and absolute;
- (6) graphical output is immediately available during the simulation run and set up in seconds;
- (7) has seven built in optimizers for excellent power in parameter adjustment to fit data;

- (8) provides the covariance matrix giving the correlation among free parameters and estimates of parameter confidence limits;
- (9) use project files that allow the analysis of many experimental data sets in one file;
- (10) stores parameter sets so that individualized parameter sets for each data set can be stored;
- (11) allows the use of several models within one project file so that competing hypotheses (models) can be compared and evaluated;
- (12) is structured so that the front end parameter control and graphical user interface (GUI) can be framed explicitly for any model;
- (13) has linear and log line graphs, 2D contour plots representing 3D, and phase-plane plots;
- (14) has "looping" capability, allowing discrete successive jumps of the values of one or two parameters at a time in order explore system sensitivities visually and rapidly;
- (15) uses a Mathematical Modeling Language, MML, in which one writes the equations directly, for simultaneous solution, and in which the order of the equations is not specified.

There are no special requirements for the JSim software or for its methods of use for model building and exploring or use in analysis with respect to hardware, computing platform, or operating system. It has important limitations, not being a procedural language but a declarative mathematical language. This means there is no equivalent of a FORTRAN DO-loop, (or GO TOs or jumps). It cannot yet do matrix inversions (except through a special mechanism), and is in a continuing state of development. JSim 2.0, released in February 2011, is based on a new compiler providing many new features described at nsr.bioeng.washington.edu/JSim/ .

The features listed above, and others not listed, have been implemented in JSim because the years of experience with a large variety of models, with teaching graduate and undergraduate classes, and postdoctoral and faculty workshops has led to a detailed understanding of how people use modeling in scientific research. Experiment design, hypothesis testing, and system parameterization are given priority in the conveniences provided.
Thus *JSim, since it is designed around the analysis of experimental data*, *is our preferred software* and will be used for the compartmental modeling shown next.

3. Compartmental Modeling

3A. The Modeling Process:

The overall process in the experiment/model hypothesis iteration loop of Platt (1964) is:
(1) express the hypothesis in quantitative terms, as a mathematical model, with units on everything; (2) use the model to determine the best experiment that might contradict the predictions of the model, or, better yet, develop an alternative model that is seemingly as good but makes different predictions, then design the experiment that clearly distinguishes between the models; (3) do the experiment and analyze the data. One of the two competing models, maybe both, must be proven wrong, and so science is advanced.

The normal data analysis using models begins by putting the data to be analyzed in a "project file", modelname.proj, and displaying them on the JSim plot-pages. The second stage, coding and model verification in accord with standards (http://www.imagwiki.nibib.nih.gov/mediawiki/index.php?title=Working_Group_10) is building and testing the model, incorporating reference analytical solutions if appropriate to verifying the solutions as being mathematically accurate and representing the equations. The "project file" may contain two or more models, so that alternative model forms can be compared directly by examining the solutions (changing parameters and rerunning, using "loops" to automatically change parameters, using behavioral analysis, plotting in various forms including phase plane plots, contour plots). The verification stage is to show that the model solutions are computed correctly, done by testing different solvers, using different time-step sizes, and comparing with analytical solutions in special cases.

The validation stage is to test the fitting of the model solutions against the experimental data. The word "validation" is truly optimistic, because a good fit of the model solution to the data does not really validate the model, but merely fails to invalidate it. It is the failure of the model that leads to the scientific advances by forcing new ideas to be incorporated. Nevertheless, fitting of the model to the data provides characterization of the data, augments diagnostic acuity, assesses progress of disease or evidence of successful therapy, and is generally useful in reconciling observations with the working hypothesis.

The final phase is preparing the model so that it can be reproduced by others. This is critical not only from a tutorial point of view, but in fact is requirement for any scientific publication. Anything that cannot be reproduced is misleading and wastes time and money. Reproducible models can be tested by others, or used as building blocks to advance the field when they pass muster.

3B. A simple compartmental model implemented in JSim:

The modeling code. For an introduction to JSim we use a 2-compartment closed system with passive exchange between the compartments, and a conversion reaction of solute A to solute B in either or both compartments. This model has analytic solutions which could be used either to show the solutions or to provide verification of the accuracy of the numerical solution, but since these solutions run no faster than the numerical solutions, they will not be used here. Detailed instruction in JSim use is available at http://www.physiome.org/jsim/ . This model is #246. Many model programs are available at http://www.physiome.org/Models. One can search to find a model similar to what one might like to construct, e.g. from a tutorial list of compartmental models: http://www.physiome.org/jsim/models/webmodel/NSR/TUTORIAL/COMPARTMENTAL/index.html . Open model #246, Comp2ExchReact, and you will be asked to allow the display on your computer, wait a moment for it to be compiled, then click on "Source" at the bottom of the JSim page to show the source code as in Figure 1. All the models on the website are archived to keep track of model changes (previous versions can be found under the 'Model History' section on each model web page). (Models edited over the web cannot be saved on the Physiome web server, so simply save what you want to your own directory. The JSim system can likewise be downloaded directly and the model worked on from your own computer.) The model for the code in Figure 1 is diagrammed at the bottom of the figure; it is a two compartment model for

two substances, A and B. Both substances can passively move from one compartment to the other. A is irreversibly converted to B in either or both compartments. After the title a short description is provided. (Text enclosed by /* …*/ is ignored by the compiler, as is comment text following // on any line.

An important JSim feature is invoked next, the reading of a units file, nsrunit, which allows automated unit balance checking and automated unit conversion to common units during the compilation phase; MKS, CGS and English units can all be used. (The unit conversion can be turned off, a feature useful when importing models from CellML or SBML which sometimes have unit conversion factors hidden as dimensionless factors in their archived models, whereas they should be dimensioned, e.g. as 60 sec/min.) The word "math" and the curly bracket designate the start of the model code, written in JSim's MML, mathematical modeling language, which will be seen to be merely the equations for the model. The "realDomain" defines the *independent* variable as *t*, time in seconds, along with a starting and ending time and a time interval for graphing the solutions.

```
/*  MODEL NUMBER: 0246
    MODEL NAME: Comp2ExchangeReaction
    SHORT DESCRIPTION: Two comparment model with two substances,
    irreversibly converting A to B.
*/
import  nsrunit; unit conversion on;

math Comp2ExchangeReaction {

// INDEPENDENT VARIABLE
realDomain t sec; t.min=0.0; t.max=60; t.delta = 0.1;

// PARAMETERS
real V1 = 0.07 ml/g,                // volume of compartment 1
     V2 = 0.15 ml/g,                // volume of compartment 2
     PSa = 1 ml/(g*min),            // Permeability Surface area product
                                    //    for exchange of A between two compartments
     PSb = 1 ml/(g*min),            // Permeability Surface area product
                                    //    for exchange of A between two compartments
     G1   = 0.0 ml/(g*min),         // Conversion rate of A to B in compartment 1
     G2   = 1.0 ml/(g*min),         // Conversion rate of A to B in compartment 2
     A10 = 1 mM,                    // initial concentration of A in compartment 1
     A20 = 0 mM,                    // initial concentration of A in compartment 2
     B10 = 0 mM,                    // initial concentration of B in compartment 1
     B20 = 0 mM;                    // initial concentration of B in compartment 2

// VARIABLES
real A1(t) mM,                      // concentration of A in compartment 1
     A2(t) mM,                      // concentration of A in compartment 2
     B1(t) mM,                      // concentration of B in compartment 1
     B2(t) mM,                      // concentration of B in compartment 2
     Equilibrium mM;                // Equilibrium concentration for B if G>0
                                    //    else for A if G=0
// INITIAL CONDITIONS
when (t=t.min) {A1 = A10; A2 = A20; B1 = B10; B2 = B20; }
Equilibrium = (V1*(A10+B10)+V2*(A20+B20) )/(V1+V2);

//ORDINARY DIFFERENTIAL EQUATIONS
A1:t = (PSa/V1)*(A2-A1)-(G1/V1)*A1;
B1:t = (PSb/V1)*(B2-B1)+(G1/V1)*A1;
A2:t = (PSa/V2)*(A1-A2)-(G2/V2)*A2;
B2:t = (PSb/V2)*(B1-B2)+(G2/V2)*A2;
} // END OF MODEL
/*

FIGURE:

    +-----------+          +-----------+
    |   G1      |   PSa    |    G2     |
    | A1---->B1 |<-------->| A2---->B2 |
    |        V1 |   PSb    |        V2 |
    +-----------+          +-----------+           */
```

Figure 1. JSim code for a two-compartment model in which a solute A can exchange across a membrane between volume V1 and V2 and can react irreversibly to form solute B in either compartment. This is available for download at www.physiome.org/jsim/models/webmodel/NSR/Comp2ExchangeReaction/index.html and is model #246.

The parameters of the model are assigned units. We have put the units in physiological form in order to represent those for a perfused tissue, so much per gram of tissue. In general it is practical to avoid mistakes by using the same units as used for the experimental studies in which the data are acquired. The volumes of the two compartments are V_1 and V_2 ml/g. In this context, flow per gram of tissue (*F*), clearances (*Cl*), and permeability-surface area products (*PS*) all have the same units, ml/(g·min). (The PS is defined as permeability, P

cm/min, times membrane surface area per gram of tissue, S cm^2/g.) The reaction is described as a clearance, but here is given the symbol G, ml/(g·min) for a gulosity or consumption. The solute A is converted from A to B. (The terminology used here is that used by the American Physiological Society (Bassingthwaighte et al 1986), where an extensive set of terms for transport, flow and electrophysiology are given.)

The model's variable are functions of the independent variable time, for example the concentration of A is defined as a real number and as a function of time by "real A(t)". In the equations A(t) can be written without the "(t)", but in JSim's MML the use of the (t) initially is required to establish it as a function of time. Other languages such as Madonna and XPPaut do not demand this, but JSim users find that this reduces errors. The MML is fairly similar to that in those languages; the basic intention is just to write the equations directly.

The ordinary differential equations, ODEs, used to describe compartmental models, need to be supplied with initial conditions, here provided as A10, A20, B10, and B20 where the first subscript digit refers the compartment and the second is "0" to refer to the initial time t =t.min, which can be negative or positive, but is usually t = 0.

In the ODEs, the derivative of A(t), which you would expect to be dA/dt is written A:t. The second derivative, d^2A/dt^2, would be A:t:t. The equations are written in state variable form in this model, for tidiness and simplicity, but this isn't FORTRAN and one could equally well write the equation as "V1*A1:t = A2* PSa – A1*(PSa + G1);". In this latter form, the left hand side, LHS, of the equation is the rate of change of mass of solute A, (moles/g)/min = mM*(ml/(g*min) for A1 in V1.

Unit Balance checking:
The acute observer will have noticed that the independent variable, t, is in seconds: the differential equation therefore looks to have unbalanced units. It actually computes correctly since the phrase "unit conversion on" at the top of the program preceding the model code, enlists the automated unit conversions, so that in the compiled code the multiplier of the left side, "60 sec/min" is inserted. Without unit conversion on, the best way to handle this is to put the independent variable *t* in minutes. In languages like Matlab there is no unit checking. In huge projects like the Mars Climate Orbiter mission (http://www.spaceref.com/news/viewpr.html?pid=2937), mixing units from the European and American programs led to the crash of the space vehicle and the termination of the billion dollar mission. There would have been no problem in JSim so long as the units were stated and unit conversion "on" (Chizeck et al 2009). The *nsrunit* file may be viewed by clicking "Debug" (left, bottom) to drop down a menu including "View system units file"). The four ODEs in Figure 1 are a complete description of the system behavior after the initial moment. Following them is an algebraic equation for TotalC, also a function of time, to check the total mass at each point in time divided by the total volume and giving the average concentration. With the initial conditions and volumes given, the result is 0.33333333 mM for every time step. Run the model and then check the numbers for the plotted variables by clicking on "Text" instead of "Graph" at the bottom of the plot page, as in Figure 2. The program end is marked by a right curly bracket, beyond which one can put notes, comments key words, diagrams, references, etc.

Graphical User Interface, GUI:

The JSim GUI for simulation control is shown in Figure 2. The left panel has overlays for project contents where all models, data sets, parameters sets, setups for solvers for ODEs and PDEs, sensitivity analysis, optimization and confidence limits. To start a simulation run one clicks "RUN" at the top of the run time window. On the right page one clicks on a "Message" panel for error messages, or the plot pages (1_Conc or 2_ReacSite, names chosen by the user), and at the page bottom choose "Graph" for displaying the output graphically or "Text" for seeing the numerical listings of the experimental data and the model solutions at each time point.

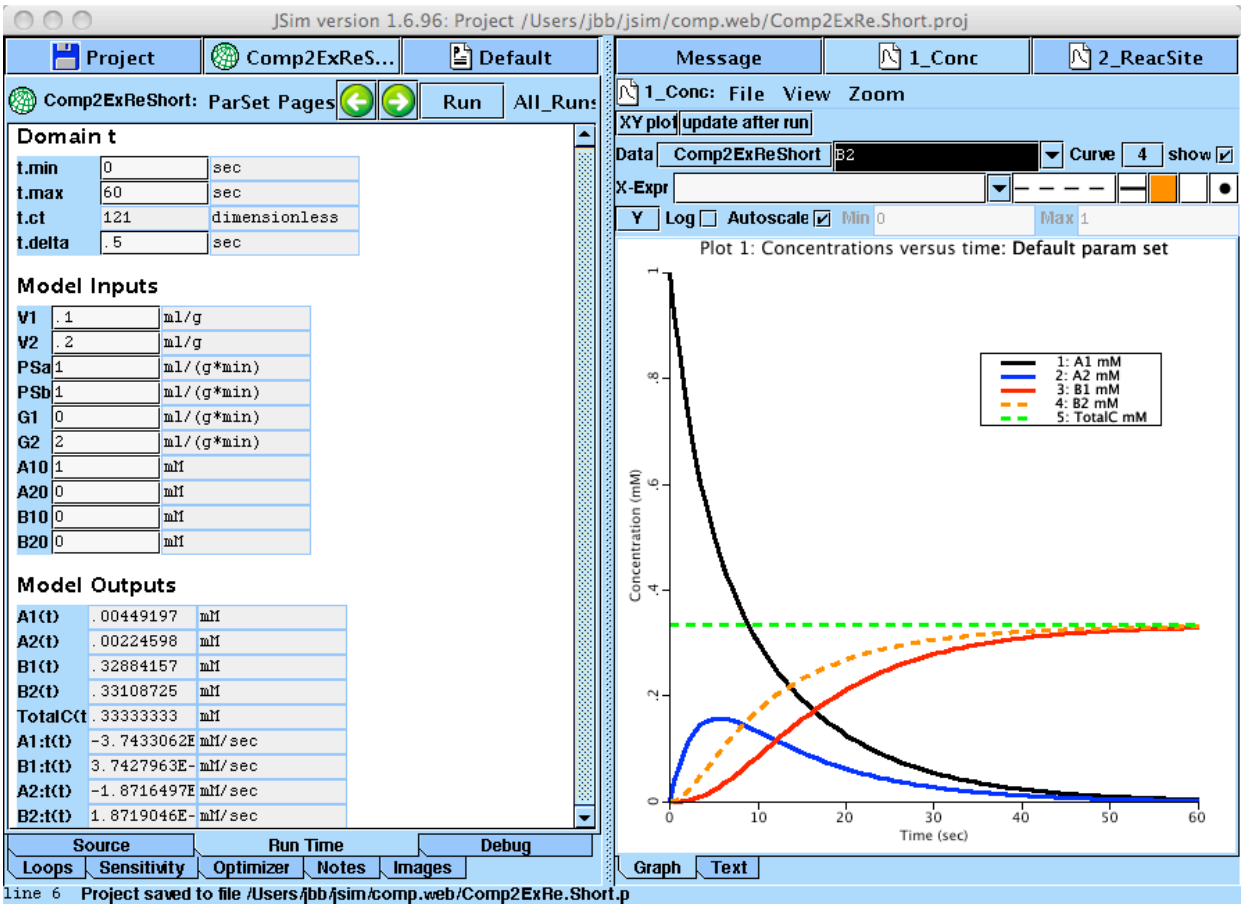

Figure 2. Standard JSim Input/Output control and plot pages. *Left panel:* Runtime control: "Domain" is time, t, with t.min starting time, t.max ending, and t.delta the time step for plotting. "Model Inputs" gives parameter values and initial conditions. Model Outputs shows values of variables at the end of the run, at t = 60 seconds. The mass balance check, TotalC, is exact to 8 decimals. *Right panel*: The time courses of concentrations and A and B in compartments 1 and 2 are shown for the parameters and initial conditions shown in the left panel and in the code in Figure 1. The user chooses the variables to plot, and the colors and line type or point type. The title and labeling are user written and retained in the JSim project file. The legend for the graphics output is automated.

There is an extensive introduction to JSim at www.physiome.org/jsim giving precise detail to supplement this outline of usage. The JSim MML code is pretty easy for a beginner to use

since it contains just the parameters with their units, the variables followed by (t) to indicate their dependence on the independent variable t for time, the initial conditions, and the equations for the model. The most common mistakes are to misapply the uses of commas and semicolons. Each of a sequence of events is usually comma separated, and a string of them is closed with a semicolon. The model code itself begins with the left curly bracket, "{" after the word "math" and ends with the right curly bracket,"}", after all of the equations have been written. Comments are preceded by a double slash, "//", or alternatively can be preceded by a "/*" followed by an "*/", without the quote signs. Equations end with a semicolon, including those in the initial condition statement.

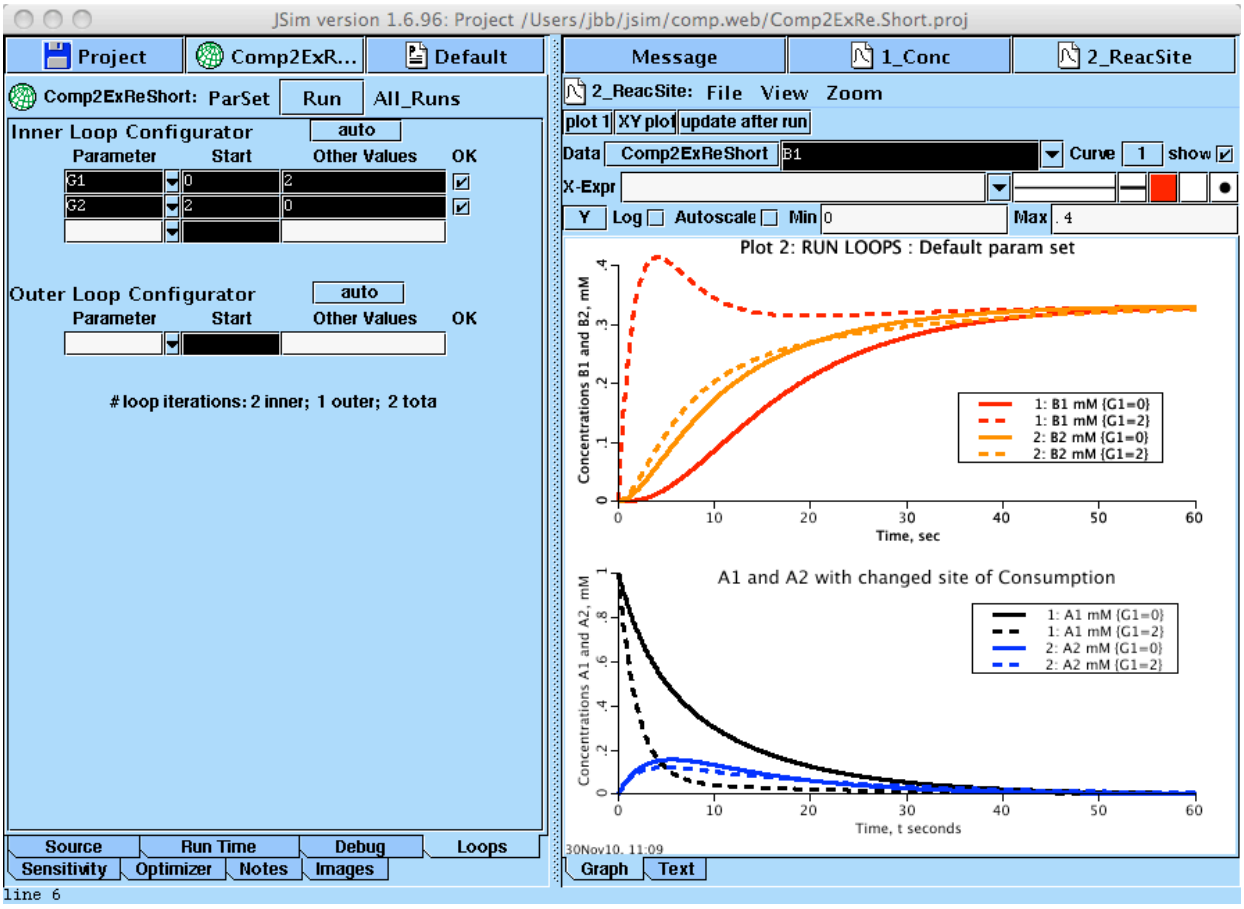

Figure 3. Loop Mode Operation. The control panel for the looping operator is shown on the left. The starting values for G1 and G2 are those shown in the code (Figure 1) and their solutions are given by the solid lines, and are the same as in Figure 2, with conversion of A → B only in compartment 1. On the second run (dashed lines of same colors) the values entered by the user under Other Values (left panel, top right) are used, in this case setting G1 = 2 and G2 = 0, so that the conversion of A → B occurs now only in compartment 1 instead of in compartment 2.

Exploring Parameter Influences using the "LOOP" mode of operation

In loop mode, the user can choose to enter a sequence of values (under Other Values) to explore model behavior widely, using comma separation, e.g. 2,3,5,8 etc., and in the "auto" mode will do as many runs as there are values entered. One can also enter arithmetic changes such as @*2 or @+3 or more complicated expressions to indicate automatic changes in the starting value by

multiplication by 2 on each run, or the automatic addition of 3 on each run, for a chosen number of runs.

Sensitivity Analysis:
Sensitivity analysis is available to provide a quantitative measure of the effect of any chosen parameter on a particular variable. This extends the information gained by "looping". The sensitivity function $S(t)$ of a variable to a parameter is calculated by calculating the change in a variable such as A(t) per fractional change in a parameter value, P. The linear sensitivity function is:

$$S(t) = \partial A(t)/\partial P, \quad [4]$$

or alternatively, the log sensitivity function is:

$$S_{log}(t) = (\partial A(t)/A(t)) / \partial P/P = \partial \log(A(t)) / \partial \log P. \quad [5]$$

Sensitivities are local linear approximations, and are calculated by computing two solutions, $A_1(t)$ and $A_2(t)$), the second having P changed by a small fraction, 0.001*P or 0.01*P, so that

$$S(t) = (A_1(t) - A_2(t)) / \Delta P , \quad [6]$$

and using the definition of the derivative as ΔP goes to zero gives the formal value.

Optimization, either by manual parameter adjustment or by automated methods, is the procedure of adjusting parameters of the equations so that the solution provides a good fit to the data. The evaluation of the goodness of fit by minimizing the sum of squares of the differences between the model solution and the experimental data is based on an implicit assumption that the differences are Gaussian random. This is seldom correct, and it is important to appreciate that the choice of the distance function is personal, i.e. it is up to the investigator to characterize the noise in the data and to weight the influence of individual data points. See next section.

4. APPLICATIONS

4A. A Compartmental Approach to Aspirin Kinetics

Aspirin is a very old drug used to reduce fever and inflammation; only recently has its mechanism of action begun to be understood, the first being its action as a blocker of prostaglandin formation. Its kinetics have not been thoroughly worked out so we present here our analysis of 3 sets of representative data from three different studies. Aspirin is acetylsalicylic acid, and its reactions are:

Acetylsalicylic acid → salicylic acid → salicyluric acid or salicyl-gluconate [7]

Aspirin, acetyl-salicylic acid is hydrolyzed quickly via a plasma esterase to salicylate. Salicylate is pharmacologically active. Salicylate kinetics dominate the clearance. The modeling examines only salicylate's enzymatic conversion to product, where product is considered to be equivalent to excretion into the urine, a saturable process. This may produce salicyluric acid or a glucuronate. The model captures the kinetics of salicylate clearance over a hundred-fold range of concentrations through consideration of one enzymatic reaction with parameters optimized to fit three very different data sets taken from the referenced papers.

The second is slow and is enzymatically facilitated. At high doses the enzyme becomes saturated, i.e. the reaction is limited by the fact that the enzyme is all in the form of the bound enzyme-substrate complex and raising the salicylate concentration does not accelerate the reaction. At low dosage the clearance is rapid; at medium or high therapeutic dosage the clearances are slower; at near lethal toxic levels clearance is very slow and often requires treatment by infusion of alkaline salts and sometimes dialysis. For this example we have taken the data from three research studies. (Low dose data are from Fig 1 Right of Benedek (1995) Dose Period 1 (squares). Medium dose data are from Fig 4 of Aarons (1995) oral dosage, last 9 points. High dose data are from Fig 1 of Prescott (1982) Control.) These particular data were chosen because the chemical methods and procedures appeared to be excellent, the data covered many hours and, while we do not have the original data, conversion from the symbols in the figures to numerical representation was accomplished with good accuracy.

A reason for choosing aspirin as the subject for compartmental analysis is that the time course of the clearance, mainly by loss into the urine, is long compared to circulatory mixing times, so that the biochemical processes appeared to limit the clearance, and they could therefore be characterized. If the circulation and distribution times were long compared to the reaction processes, the latter would not be meaningfully determined from the observations. Another reason was that a comparison among the different data sets suggested that the clearance was enzymatically mediated: at high concentration the diminution was almost linear, at low concentrations it was almost exponential, and at intermediate concentrations the rate of clearance appeared to speed up with time. This fits the expectations for a *saturable enzymatic process*: at low concentrations well below the dissociation constant for the enzyme substrate complex almost all of the enzyme is free and available for the reaction and therefore the fractional transformation of substrate is at its highest. With all the enzyme free this is a first-order process, a single exponential. In contrast at high concentrations the enzyme is almost totally saturated and the conversion is at a maximum rate independent of the concentration; this is zero order kinetics, giving a linear diminution in concentration. Thus the shift from zero order kinetics to what occurs at intermediate concentration, a gradually increasing fractional rate of reaction, is what was suspected by looking at the middle level concentrations.

Thus we hypothesize an enzyme conversion model for salicylic acid clearance, and then test the surmise by attempting to simultaneously fit the three independent data sets using one set of parameters. To do this in one program and to optimize the fit to the data for all three salicylate levels we coded three identical models in the one program. These are computed simultaneously in order to fit the three independent data sets from the three research reports using *one common set of parameters*, and automated optimization was used to minimize the set of differences between data and model solutions.

The reactions, both the binding to the enzyme and the product formation, are reversible:

$$SA + E \underset{k_{off1}}{\overset{k_{on1}}{\rightleftharpoons}} SAE \underset{k_{on2}}{\overset{k_{off2}}{\rightleftharpoons}} E + P \qquad [8]$$

The equations and parameters are identical for the three dosage levels. Here is the model code for the low dose, where the prefix L distinguishes this model equations from those for the medium dose, prefixed M and the high dose, prefixed H, neither of which are shown in Table 2:

Table 2. Model code for salicylate clearance
(Model downloadable from www.physiome.org/Models: search for model 280)

```
/* MODEL NUMBER 280
   MODEL NAME: Aspirin
   SHORT DESCRIPTION: Salicylic acid (SA) clearance for three different
   dose ranges is modeled as an enzyme reaction. This table is abbreviated by omitting the code for the Mid
and High dose reactions.)
 */
 import nsrunit; unit conversion on;
 math Aspirin {

 // INDEPENDENT VARIABLE
 realDomain t hour; t.min=0; t.max=16.0; t.delta=0.05;

 // PARAMETERS (SAME FOR ALL THREE MODELS)
 real konl  = 0.174 L*mg^(-1)/hour,   // On rate for SA + enzyme
    KD1   = 6.3   mg/L,               // Dissociation constant for SA enzyme complex
    koff1 = KD1*konl,                 // Off rate for SA enzyme complex
    kon2  = 0.003 L/(mg*hour), // On rate for Product + enzyme
    KD2   = 250 mg/L,                 // Dissociation constant for Product enzyme complex
    koff2 = KD2*kon2,                 // Forward rate to form Product from complex
    Gp    = 0.03 l/hour,              // Clearance rate from plasma
    Etot  = 10 mg/L;                  // Total enzyme concn

 // LOW DOSE MODEL: Data from Benedek (1995) Fig 1 Right Dose Period 1 (squares)
 //    LOW DOSE PARAMETER
 real LSAtot = 7.9 mg/L,              // Total Low Dose concentration
 //    LOW DOSE MODEL VARIABLES
    LSA(t)  mg/L,                     // Low dose SA
    LSAE(t)  mg/L,                    // Low dose SA-enzyme complex
    LE(t)  mg/L,                      // Low dose free enzyme
    LP(t) mg/L;                       // Low dose product
 //    LOW DOSE INITIAL CONDITIONS
 when(t=t.min) {LSA=LSAtot; LSAE=0; LP=0;}

 //    LOW DOSE ORDINARY DIFFERENTIAL AND MASS BALANCE EQUATIONS
 LSA:t = -konl*LSA*LE+koff1*LSAE;
 LSAE:t = konl*LSA*LE-koff1*LSAE-koff2*LSAE+kon2*LE*LP;
 LP:t   = koff2*LSAE - kon2*LE*LP - Gp*LP;
 LE     = Etot - LSAE;                 // LSAtot = LSA+LSAE+LP; for an overall mass balance accounting

 }  //End of Low Dose Model. The omitted code for the medium and high dose models is identical
   // but L is replaced with M or H. Copy and paste the Low Dose Model  into the space preceding the
   // right curly bracket, twice,  and change the L to M for one copy, and L to H for the other; recompile.
```

++++++++++++ End of Table 2 ++++++++++++++++++++++++++++++++++

In undertaking an analysis on a single enzymatic reaction we lack knowledge of the exact mechanism. In addition the compartmental approximation is certainly questionable for whole body studies. The hypothesis that a single enzymatic reaction dominates the clearance would be strengthened if the model provides good fits to the three data sets. There is no guidance from the literature on the dissociation constant, K_D, for our presumed enzymatic reaction, so that we are neither constrained nor aided.

We chose to use a simple enzymatic reaction, one that allowed characterizing the rates of binding and unbinding of substrate and enzyme, and a rate of the forward reaction to yield the product. We allow also a backward reaction, on the basis that *all reactions are thermodynamically reversible*, at least in principle. This reaction set up allows reduction to the simpler, commonly-used Michaelis-Menten reaction; this is accomplished by speeding up the binding and unbinding reactions of salicylate to enzyme and eliminating the reverse reaction from the product back to salicylate. So for the first level of testing all parameters are considered as open and adjustable, including the initial values of the concentrations in the system. In this analysis the system is considered to be a single well stirred tank, as if the circulation were instantaneously mixed. This gross oversimplification also makes the assumption that the product either goes directly into the urine or to some other location in the body from which it does not return. Enzymatic conversion in the liver followed by excretion into the bile would be equivalent kinetically to conversion to a glucuronate followed by the circulation through the blood and clearance in the kidney. Ideally one would measure the urinary excretory rates simultaneously and model both the plasma clearance rates and the urinary clearance. This was not done here.

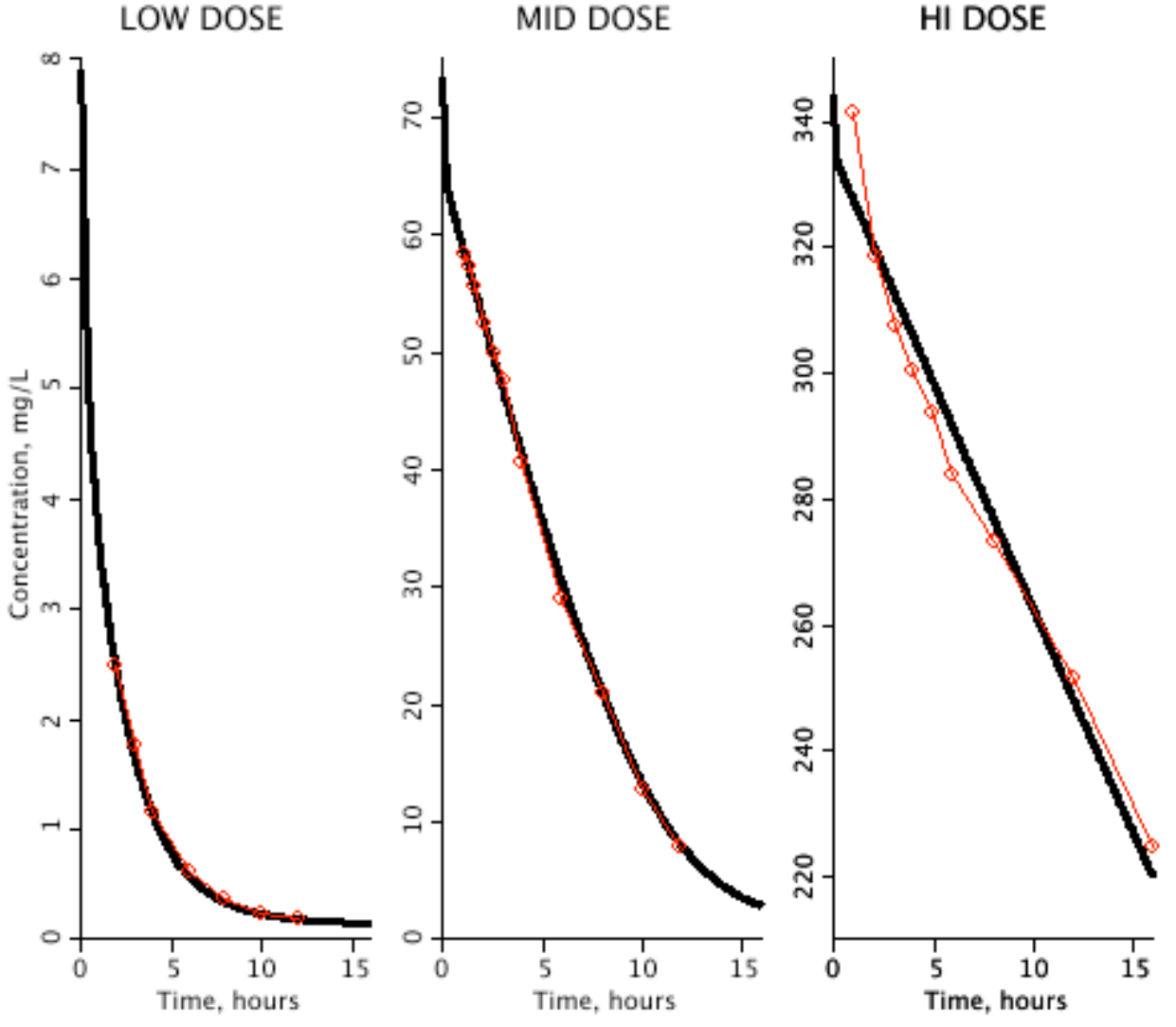

Figure 4. Data on salicylate clearance from the three laboratories are fitted simultaneously with a single enzyme model to describe the clearance. Parameters are given in the model code in Table 2. Data are from Benedek (1995) in the left panel, Aaron (1989) in the middle panel, and Prescott (1982) in the right panel. Note that the concentration ranges are markedly different. (http://www.physiome.org/jsim/models/webmodel/NSR/Aspirin/)

The results are shown in Figure 4 where the curves at the low, middle, and high concentration ranges are shown to be fitted reasonably well by the model. The high concentration data (right panel) are fitted less well and but do illustrate that the slope is approximately linear, as expected, whereas at the low concentrations (left panel) the curve is nearly exponential, as expected.

A different view is provided by Figure 5, a semilog plot of the three sets of data each fitted by the model. The high concentration curve (open circles, purple line) appears to be almost linear on this plot, but the slope is shallow, and judgment based on Figure 4 is better. The high dose concentrations are very much higher than the K_{D1} for substrate binding, estimated at 6.3 mg/L, so that there is no doubt that the enzyme was almost saturated. In fact, with the High Dose the concentrations are above apparent K_{D2} of 250 mg/L for product binding so there is significant reversal of the reaction. At Mid Dose level (triangles, blue line) the slope diminishes as time progresses, that is to say the fractional clearance is increasing as the enzyme becomes less saturated. The Low Dose data (diamonds, green line) are fitted well and have considerable curvature on the semilog plot, the slope at late times being much diminished: this leads to the idea that there is some tendency for retention at the low concentrations, which could be either due to recirculation from other parts of the body where the concentrations were initially higher or there is "product pressure" to form salicylate by the reverse reaction. The reversibility is governed by the K_{D2} for the product, which here was about 250 mg//L. There must be even more reverse flux with the middle and higher-level concentrations, HP and MP, a feature of product inhibition, and the estimate of this K_{D2} is determined from both of these, even though the effect is most evident from the curvature of the low salicylate dose, LSA.

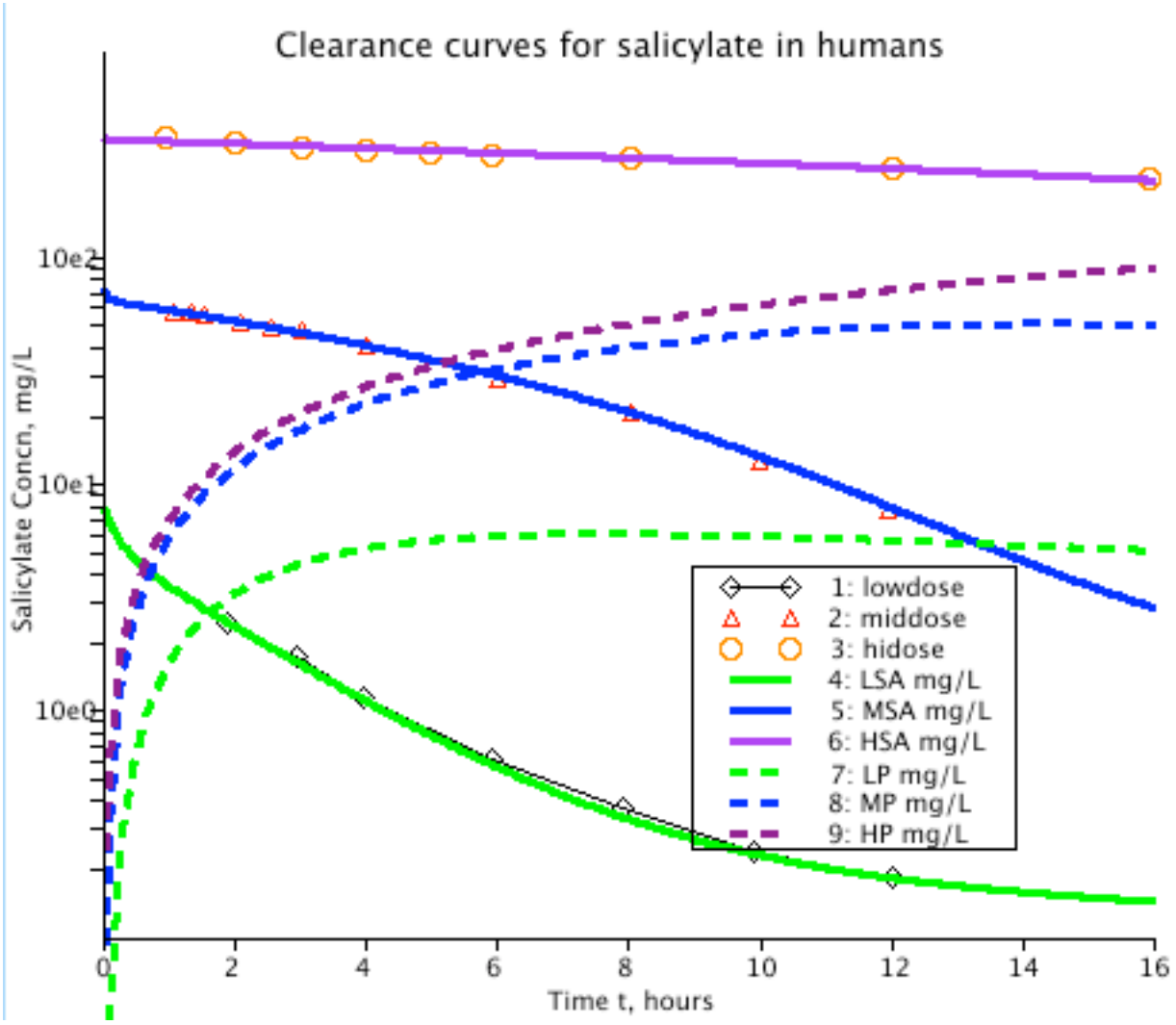

Figure 5. Semilog plots of the data (symbols) and model solutions (LSA, MSA, and HSA, solids lines), and the predicted Product concentrations (LP, MP, and HP). There are no data to check on the product concentrations; the predicted product concentrations are based on the assumption that all Product remains available to the enzyme, which is certainly an overestimate.

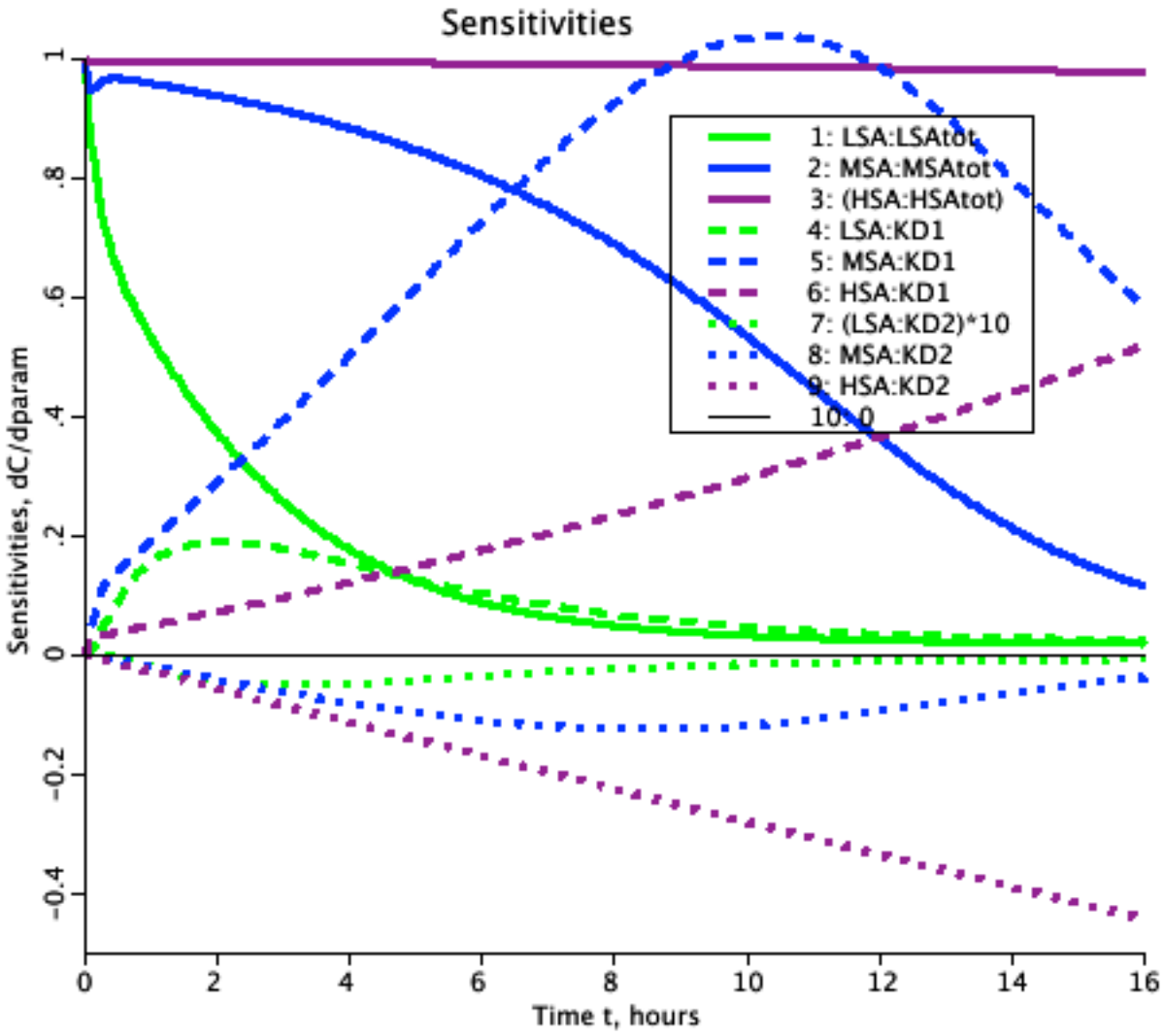

Figure 6. Three sets of linear sensitivity functions versus time. ***Solid lines*** are sensitivities to the initial zero-time concentrations resulting from the doses. ***Long dashed lines*** are sensitivities to K_{D1}: the sensitivities are all positive. ***Dotted lines*** are sensitivities to K_{D2}, the dissociation constant for the reverse reaction: the sensitivities are all negative.

Sensitivity Analysis:

In Figure 6 the linear or absolute sensitivity functions are shown for initial concentrations and for the two dissociation constants. The ***solid lines*** are sensitivities to the initial zero-time concentrations resulting from the doses; most of the sensitivity is at the earliest points. With the high dose the fractional clearance is so low that the high sensitivity extends throughout the 16 hours of the study. For the middle dose, MSAtot, the sensitivity diminishes most steeply as a function of time at around 10 hours when the concentration is close to K_{D1}, the dissociation constant for substrate binding. The ***long dashed lines*** are the sensitivities to K_{D1}; these are all positive, meaning that if K_{D1} were increased (decreasing the affinity of the enzyme for the substrate SA) the model solutions for all three doses would be at higher levels and the rate of disappearance would be diminished. Note that the time of peak sensitivity to K_{D1} is at early times for the low dose, at 10 hours for the middle dose and at late times for the high dose. The ***dotted lines*** are sensitivities to K_{D2}: the sensitivities are all negative, meaning that if K_{D2} were increased

(decreasing the affinity of the enzyme for the product P) the model solutions would be at lower levels *and the rate of disappearance would be increased* because of reduced rates of reverse flux from product to salicylate.

Technically the sensitivity calculations are set up by a special mechanism: at the bottom of the left page is a button labeled "Sensitivity". Clicking on it takes one to the "Sensitivity Analysis Configurator". There in the left most column of the configurator table one types in, or chooses from the drag down menu, the parameter for which one wants to find the sensitivity. By clicking on the down arrowheads you bring up the choices. In the set up provided on the website at www.physiome.org etc. the three starting values for the initial concentrations at t = 0 are listed: LSAtot, MSAtot and HSAtot. Next on the list are the dissociation constants K_{D1} and K_{D2}.Their current values are automatically displayed under "value". The calculations of each S(t) are made on the basis of the parameter change of 1% set under "delta" at 0.01. The tick marks in the OK column indicate that the calculation will be made as described earlier, namely that the standard solution will be calculated and then another solution calculated for each of the five parameters listed, with this 1% change in parameter value. The *S*(t) is the difference in the solution at each time point from the standard solution divided by the 1% change in the parameter value, Eq. 4.

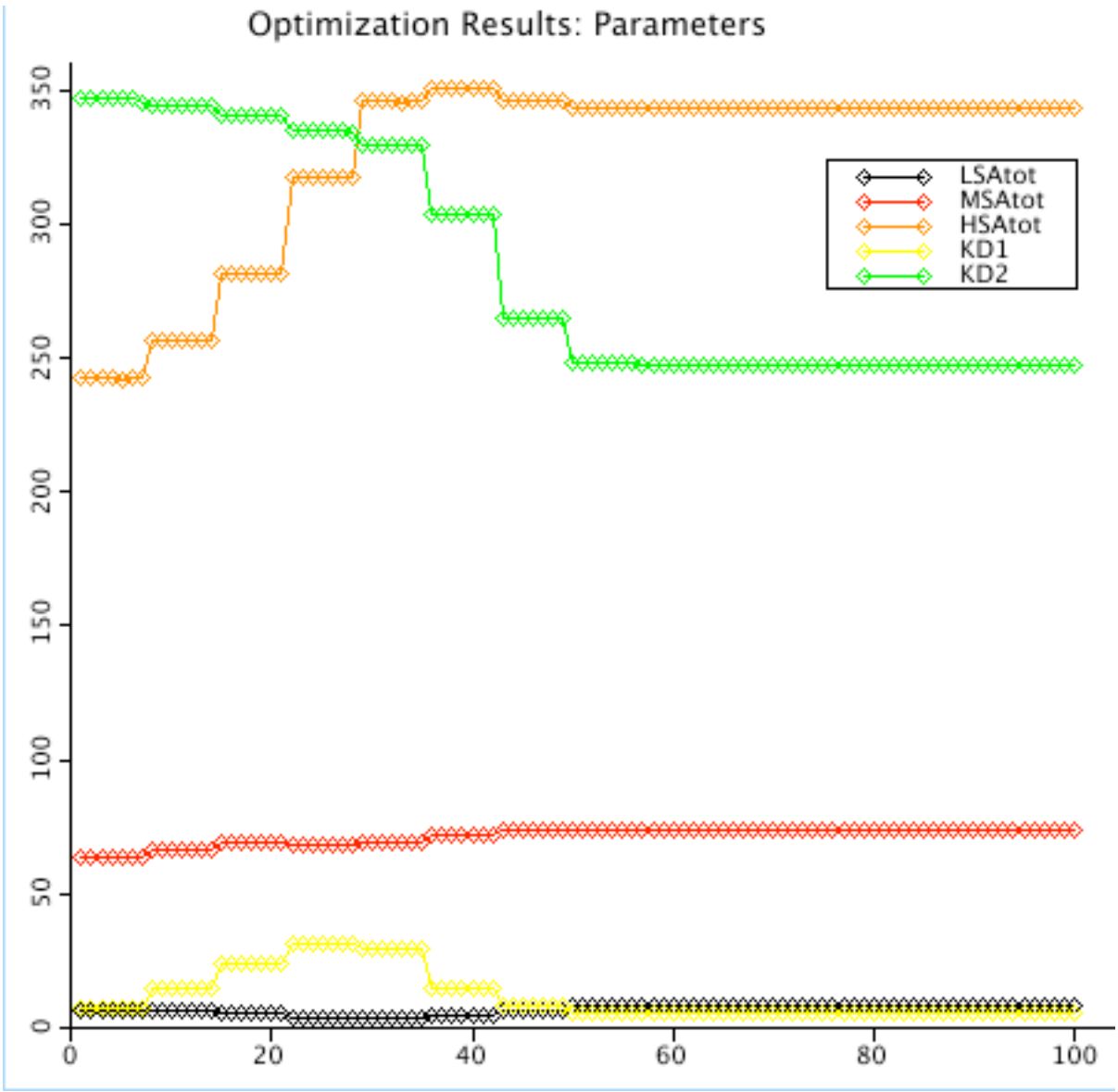

Figure 7. Optimization: Trajectories of values for parameters being optimized, in this case the three initial concentrations and the two dissociation constants during 100 trials of fitting the model solutions to the data. The optimizer used was SENSOP (Chan 1993); the staircase nature of the plotted values is that SENSOP reports the previous estimate of the parameter vector as it calculates each new sensitivity function, one for each parameter being optimized, and then reports and plots the new value of each parameter.

Optimization: This is the process of fitting the model solutions as closely as possible to the data in order to guide one's thinking about, and one's use of the model. When the fit is very close, then one has a descriptor of the fitted data sets, that is, the model and its parameter set provide a record of that description. Descriptions of many different studies, patients studies or experiments, allow comparisons and possible classification into categories having specific distinctions. Descriptive models are useful for diagnosis and possibly for prognosis or choosing modes of therapy. (If the model "explains" the data by defining the physical and chemical mechanisms, that is even better.)

When the fit is poor, then more exploration is needed. Was automated optimization used? If so, then try other optimizers. Try weighting the data differently: a simple sum of squares

minimization may not be appropriate; it is almost never appropriate if the data range over one order of magnitude. For example when fitting a decay process that is exponential, one can use a reciprocal weighting, so that points are weighted more evenly, or a weighting adjusted to the individual result such as "1/exp(-t/(2 hour))" for the low dose data set, and "1/exp(-t/(8 hour))" for the middle dose data. These choices of weighting are to be typed, without the quotes, into the appropriate line under Pwgt (point weighting) in the Data to Match Table on the Optimizer Configuration Page.

In the same table there is opportunity to even up the weightings for the three quite different curves by using Curve Weighting, Cwgt. In this case we weighted Low Dose data with 140 times the weight of the High Dose Data since the latter were about 140 times higher concentrations, thereby evening up the weighting the contributions to the sum of squares. Likewise the Middle dose data were weighted at 14, that is, about 10 times higher than the High Dose data. This combination of Point weighting within each data curve, and Curve weighting among the three data curves gives each point in the triple data set about the same weight. This makes the calculation of a root mean square error provided by the minimization of the sum of squares a reasonable strategy. This is probably close to what one would do if using "eyeball best fitting", examining the fitting to all the points. Both Figure 1 and Figure 2 plots are valuable in this regard since they weight the curves differently from the "eyeball" view. While arguing that the eyeball fitting is just as valid as that from automated optimization, the latter has the virtue that the weighting scheme is explicitly stated, and that the weighted sum of squares can be reproducibly reported when the weighting scheme is reported also.

There are situations where an optimizers fails to reach a good fit because the sum of squares has settled in a local minimum. Optimizers like Gridsearch and Simulated Annealing are designed to cover a wide range in state space, so that even the corners get explored. Others like SENSOP, GGOPT and NL2SOL make excursions, jumping out of the locale to test other regions for a better fit. To switching optimizers, simply pick another one from the drag down menu.

4B. Multiple sequential dose administration: Hepatic function

Test of clinical functions evolve in a variety of ways, usually being designed long after the function has been clearly understood. Here's a counterexample, a case in which the idea of the clinical evaluation from the administration of a drug was evident right at the beginning. There was a coalescence of features that brought this about.

For the estimation of cardiac output using the indicator dilution technique Mayo Clinic's Earl Wood needed a dye that absorbed light at a wavelength of 800 nm, the isosbestic point at which oxyhemoglobin and reduced hemoglobin absorbed equally. This would allow optical detection and quantitation of the dye concentration independent of the blood oxygen level. The dye, indocyanine green, was found in Kodak's repository (Fox, 1957); it was not toxic; its absorbance peaked at 805 nm; it bound to albumin and so stayed in the circulation and did not color the body. The densitometer measuring the absorbance was developed (Edwards 1963), and a spin-off from it was an earpiece densitometer that could be used to detect blood concentration non-invasively. In early experiments to test the accuracy and reproducibility of the estimates of cardiac output, dye was injected repeatedly as a bolus into a vein and the arterial concentration-time curve recorded each time. The repeated injections led to a rise in the background arterial concentration, raising the question of whether the detector could be calibrated accurately over a

large range of concentrations (Edwards, 1960; Bassingthwaighte, 1966a). In the first studies, we found right away that the dye was excreted via the bile: the feces turned green! Within a few years the Indocyanine Green clearance Test was used a liver function test; it was a valued test even before the mechanisms of its hepatic excretion became known (Hunton 1961).

The data from one dog (Edwards, 1960), shown in Figure 8 (top panel) invite analysis. After each series of injections a set of blood samples were obtained as the concentration diminished: the diminutions appeared as straight lines on the semilog plot shown in Figure 8, top. This suggests a first order clearance, i.e. a constant fraction of the dye was being removed per unit time. Now let us develop a simple model, and then test it against the data.

The anatomy and physiology provide the framework for the model. The dye distributes throughout the whole blood volume. We hypothesize that it is removed at one point only, by the liver, and is excreted into the bile. We have no data on biliary concentration versus time, except that the dye ends up in the lower bowel within the duration of the experiment, 4 hours. We model the quantitative data: the doses and their time of injection, the blood concentrations at the particular times, and use the dog's weight, 14 kg, as a constraint. The cardiac output is known from the areas of the dye-dilution curves: C.O. = Dose injected (mg) / Area under dye curve (min. mg/L). These averaged 1.5 L/min, with a standard deviation of about 10% (Bassingthwaighte, 1962).

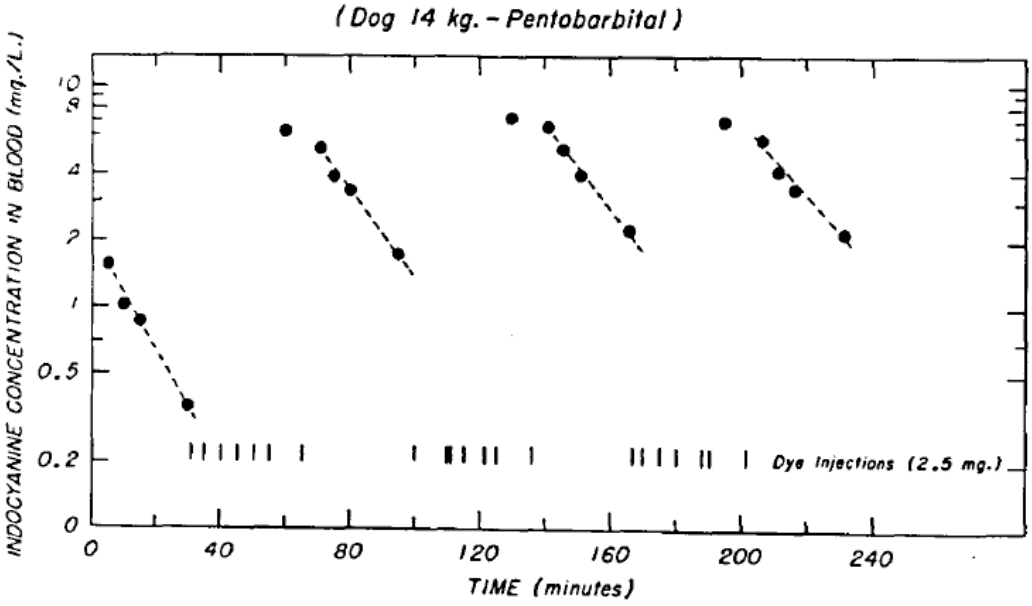

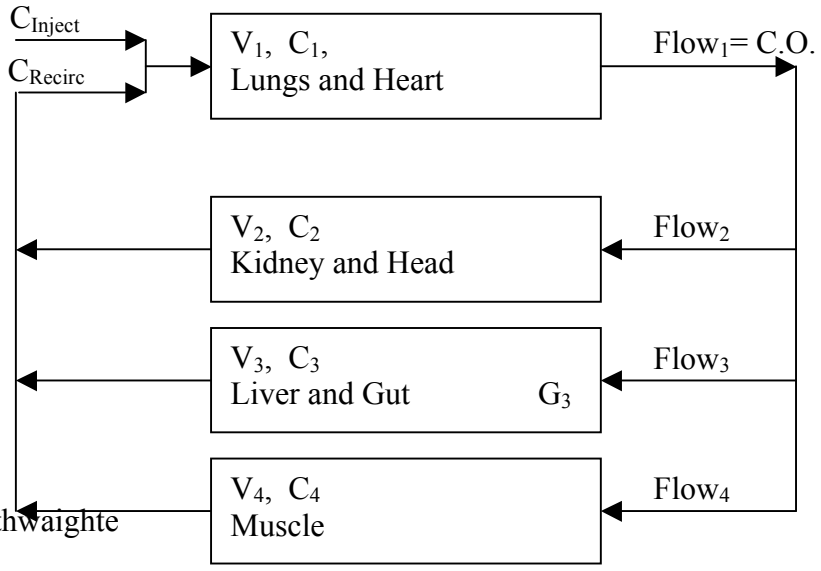

Figure 8. Indocyanine Green Injection and Clearance. *Upper Panel*: Blood concentrations in a 14 Kg dog with 22 successive intravenous injections of 2.5 mg ICG (vertical pips). Dashed lines represent estimated single exponential decay after each series of injections. Data are from Edwards et al. 1960. *Lower panel:* Circulatory model for hepatic clearance of ICG, a mammillary compartmental model. Model code, with all parameters and equations, is in Table 3. Modeling results are in Figure 9.

A simple model of the whole body circulation is chosen as a compromise, a three compartments to represent fast, moderate, and slow flows throughout the body and a single lumped compartment to represent blood in the heart and lungs, as in Figure 8, lower panel. A mammillary model of this sort is far too crude to represent the indicator dilution curves used to measure the cardiac output; this requires higher temporal resolution (Stewart 1890; Hamilton, 1932) and more precise models (Thompson 1964; Bassingthwaighte, 1966b). In this model there are up to three parameters for each of the four compartments, flow and volume, and in compartment 3, a consumption term G_3. The shape of the transport function is fixed by the assumption of a mixing chamber, so each has the impulse response $h(t) = (1/\tau)\ \exp(-t/\tau)$, where the time constant τ = volume/flow. The consumption influences the fraction leaving the compartment. If we were to try to use the observed concentrations in Figure 8 upper as the input to the model we'd see at once that we don't have enough data: the points sampled are too sparse.

But the doses and their times of injection are precise, so we use the sequence of doses as the input. We represent the process of flow distribution and dilution of the injected ICG by the set of 4 first order differential equations, stirred tanks, as in traditional compartmental analysis. Within each tank the concentration, C_i, is given by:

$$dC_i/dt = (F_i*(Cin_i - C_i) - G_i*C_i) / V_i, \qquad [10]$$

where the index subscript i denotes the compartment, F is its flow, V is its volume, and G is the rate of consumption within the volume. Cin_i is the concentration in the blood entering the volume, and equals the concentration in the compartment just upstream. The concentration C_i is the same as the concentration flowing out, because the basic compartmental assumption that the tank is stirred instantaneously from entrance to exit. Via the test of fitting the model to the data we can assess whether or not this assumption is refuted by the data; if the data are fitted, then we do not prove that the assumption is correct, but only that it was not invalidated by the data. (This philosophical point underlies every assumption in formulating a model: a model can never be proven correct. It can only be demonstrated as adequate for the situation, and then can be used as a "working hypothesis", yet to be disproven. As T. H. Huxley put it: "The great tragedy of science: the slaying of a beautiful hypothesis by an ugly fact." The downfall leads to the advancement!)

The JSim code is given in Table 3. The equations for each compartment are closely similar. The recirculated dye and newly injected dye enter the heart and lung compartment with central blood volume V_1, and mix with the total cardiac output. The only clearance, G_3, is during passage through the liver where ICG is highly extracted and secreted into the bile; G_2 and G_4 are available for exploration, but are set to zero.

TABLE 3. Compartmental Model for Hepatic ICG Clearance

```
/* MODEL NUMBER: 0103
   MODEL NAME: Comp4ICG
   SHORT DESCRIPTION: Four-compartment whole body model with recirculation:
Repeated injections and first-order hepatic clearance of Indocyanine Green dye. */

import  nsrunit; unit conversion on;
math Comp4ICG {

// INDEPENDENT VARIABLE
realDomain t min; t.min=0; t.max=30; t.delta=0.1;

// PARAMETERS
real  Flow1 = 1.5 L/min,        // Blood Flow through Heart/Lung = Cardiac Output
       Dose = 2.5 mg,             // Amt injected
       Vtot  = 1. 256 L,          // Total Blood Volume
// First Compartmental unit (Heart/lung)
      Vfr1 = 0.25 dimensionless, // fraction of Vtot in Comp 1
      V1   = Vfr1*Vtot,          // Volume of blood 1
      C10  = 0 mg/L,             // Initial concentration
// Second Compartmental unit (Kidney and Head)
      Fr2     = 0.33,            // Fraction of flow through comp 2
      Flow2 = Fr2*Flow1,         // Flow through Comp 2
      Vfr2   = 0.40,             // fraction of Vtot in Comp 2
      V2     = Vfr2*Vtot,        // Volume of blood 2
      C20   = 0 mg/L,            // Initial concentration
      G2     = 0 ml/min,         // consumption 2
// Third Compartmental unit (Liver and Gut)
      Fr3     = 0.25,            // Fraction of Flow through Comp 3 (Liver)
      Flow3 = Fr3*Flow1,         // Flow through Comp 3
      Vfr3   = 0.25,             // fraction of Vtot in Comp 3
      C30   = 0 mg/L,            // Initial concentration
      G3     = 63.7 ml/min,      // comsumption 3
// Fourth Compartmental unit (Muscle)
      Fr4   = 1 - Fr2 - Fr3,     // Fraction of Flow through Comp 4
      Flow4 = Fr4*Flow1,         // Flow through Comp 4
      Vfr4  = 1 -Vfr1 -Vfr2 -Vfr3, // fraction of Vtot in Comp 4
      V4    = Vfr4*Vtot,         // Volume of blood 4
      C40   = 0 mg/L,            // Initial concentration
      G4   = 0 ml/min;           // Comsumption 4

// Total flow relationship:  Flow4 = Flow1 - Flow2 - Flow3;

// EXTERNAL VARIABLE: The series of ICG injections, 2,5 mg each
extern real Cin1(t) 1/min;      // 60 second Pulse injection @ 0.1 min
extern real Cin2(t) 1/min;      // 60 second Pulse injection @ 30 min
extern real Cin3(t) 1/min;      // 60 second Pulse injection @ 34 min
extern real Cin4(t) 1/min;      // 60 second Pulse injection @ 39 min
extern real Cin5(t) 1/min;      // 60 second Pulse injection @ 44 min
extern real Cin6(t) 1/min;      // 60 second Pulse injection @ 49 min
extern real Cin7(t) 1/min;      // 60 second Pulse injection @ 54 min
extern real Cin8(t) 1/min;      // 60 second Pulse injection @ 64 min
extern real Cin9(t) 1/min;      // 60 second Pulse injection @ 99 min
extern real Cin10(t) 1/min;     // 60 second Pulse injection @ 109 min
extern real Cin11(t) 1/min;     // 60 second Pulse injection @ 110 min
extern real Cin12(t) 1/min;     // 60 second Pulse injection @ 114 min
extern real Cin13(t) 1/min;     // 60 second Pulse injection @ 120 min
extern real Cin14(t) 1/min;     // 60 second Pulse injection @ 124 min
extern real Cin15(t) 1/min;     // 60 second Pulse injection @ 135 min
extern real Cin16(t) 1/min;     // 60 second Pulse injection @ 165.9 min
extern real Cin17(t) 1/min;     // 60 second Pulse injection @ 168.8 min
```

```
 extern real Cin18(t) 1/min;       // 60 second Pulse injection @ 174.1 min
 extern real Cin19(t) 1/min;       // 60 second Pulse injection @ 179.3 min
 extern real Cin20(t) 1/min;       // 60 second Pulse injection @ 186.9 min
 extern real Cin21(t) 1/min;       // 60 second Pulse injection @ 189.6 min
 extern real Cin22(t) 1/min;       // 60 second Pulse injection @ 200.8 min

 // DEPENDENT VARIABLES
 real Crecirc(t) mg/L,        //Inflow + recirculation
     Qtot(t) mg,              // Total amt in 4 compartments
     Cinsum(t) 1/min,         // Sum of the string of pulse injections
   // Comp1          Comp2     Comp3          Comp4
     C1(t) mg/L,  C2(t) mg/L,   C3(t) mg/L,  C4(t) mg/L,    // concn in each region
     Q1(t) mg,    Q2(t) mg,     Q3(t) mg,    Q4(t) mg;      // Quantity in each regions

 // INITIAL CONDITIONS
 when(t=t.min) {C1 = C10; C2  = C20; C3 = C30; C4 = C40;}


 // INPUT CONCENTRATION FUNCTION
 real Qinjrate(t) mg/min;
 Cinsum = (Cin1+ Cin2 + Cin3 +  Cin4 +  Cin5 +  Cin6 +  Cin7 +  Cin8+
             Cin9+ Cin10+ Cin11+ Cin12+ Cin13+ Cin14+ Cin15+
           Cin16+ Cin17+ Cin18+ Cin19+ Cin20+ Cin21+ Cin22);
 Qinjrate = Dose*Cinsum;
 Crecirc = (C2*Flow2+ C3*Flow3 + C4*Flow4)/Flow1;

 // QUANTITY Retained at time t:
 Qtot = V1*C1 + V2*C2 + V3*C3 + V4*C4  // Qtot is the total amount of ICG in the body at time t.

real Area = Dose*(integral(t=t.min to t.max, Cinsum)); // check amt injected

 // ORDINARY DIFFERENTIAL EQUATIONS
 V1*C1:t   =  Flow1*(Crecirc-C1) + Cinject;  // Note that V1 can be left of = sign
 C2:t   =  Flow2*(C1-C2)/V2 - G2*C2/V2;
 C3:t   =  Flow3*(C1-C3)/V3 - G3*C3/V3;
 C4:t   =  Flow4*(C1-C4)/V4 - G4*C4/V4;

 } // END of program
 /*
    DETAILED DESCRIPTION:
This is a whole body model composed of a central blood volume from which flows
 the whole cardiac output. The C.O.is distributed into three organs labeled "kidney"
 for kidney and head,"liver", for liver and intestines, and "muscle" for the rest of the body.
 The four compartment model has recirculation. The input function to compartment 1
 (Heart and Lung) is the sum of the recirculated indicator plus the series of injection
 pulses into V1, Qinjrate, each injection at x mg/min for a short duration. Each injection,
 Cin#, is defined at run time using a separate function generator. Clearance of the
 injected dye, indocyanine green, is hepatic extraction from the blood via a saturable
 transporter on the hepatocyte sinusoidal membrane followed by ATP-dependent excretion
 across the hapatocyte apical membrane into the bile, but is represented here by a
 passive first order loss, G3. This is adequate kinetically only at low concentrations
 of ICG, where the transporter is mainly uncomplexed.                */


 KEY WORDS: compartment, flow and exchange, mixing chamber, hepatic
clearance. first-order consumption, washout, organ, multi-organ, recirculation

 REFERENCES:
   Edwards AWT, Bassingthwaighte JB, Sutterer WF, and Wood EH. Blood level of indocyanine green in the dog
during multiple dye curves and  its effect on instrumental calibration. Proc S M Mayo Clin 35: 747-751, 1960.
   Edwards AWT, Isaacson J, Sutterer WF, Bassingthwaighte JB, and Wood EH. Indocyanine green densitometry in
flowing blood compensated for background  dye. J Appl Physiol 18: 1294-1304, 1963.
```

```
REVISION HISTORY:
        Author :      BEJ  06jan11
        Revised by: JBB   09jan11 to combine the function generators, fgens, to speed computation

COPYRIGHT AND REQUEST FOR ACKNOWLEDGMENT OF USE:
 Copyright (C) 1999-2011 University of Washington. From the National Simulation Resource,
 Director J. B. Bassingthwaighte, Department of Bioengineering, University of Washington, Seattle WA 98195-5061.
 Academic use is unrestricted. Software may be copied so long as this copyright notice is included.
 This software was developed with support from NIH grant HL073598.
 Please cite this grant in any publication for which this software is used and send an email
 with the citation and, if possible, a PDF file of the paper to: staff@physiome.org.
*/
```

……. End of Table 3 …….

Table 3 is an example of a complete set of MML code in the format used in general for JSim project files, having the same sequence and format as those used in the repository of models at www.physiome.org/Models.

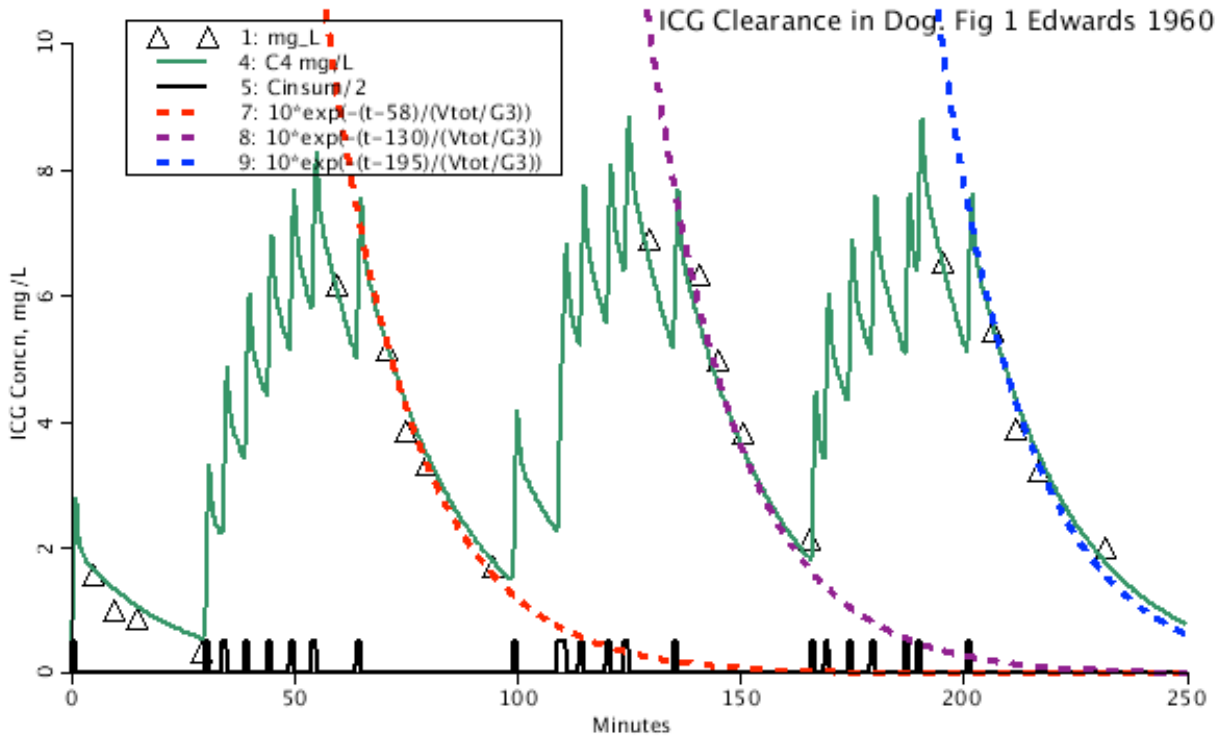

Figure 9. Model solution to fit the ICG data in a 14 kg dog. The triangles are the data shown in Figure 8 (upper). The parameters and initial conditions for the model are those given in the code in Table 3. The parameters are the result of optimization using NL2SOL from Dennis and Schnabel (1983); the total blood volume, V_{tot}, and the hepatic clearance, G_3, were the only free parameters. The 2.5 mg injection pulses are shown along the abscissa. The dashed lines are mono-exponentials with time constant V_{tot} / G_3. The model is #103 at http://www.physiome.org/jsim/models/webmodel/NSR/Comp4ICG/ .

The modeling results are shown in Figure 9. Each injection resulted in a sharp rise in concentration; when closely spaced the mean concentration rises in spite of the rapid clearance. In the absence of injections the concentration diminishes almost mono-exponentially as was suggested by the straight lines on the semilog plot in Figure 8 (upper). If the system were a

perfect single mixing chamber with first order clearance the time constant for washout would be the volume divided by the clearance, V_{tot}/G_3, and in fact this is very close. The test is to plot the theoretical concentration diminution against the model and the data. The equation,
Test = 10*exp(-(t-58)/(V_{tot}/G_3)),
is the red dashed line in Figure 9, and it does fit the phase where there are no injections after 64 minutes and before the next injection at 100 min. The multiplier, 10, and the delay, 58 min, in the equation simply position the curve. Test curves with longer delays (130 and 195 minutes for the purple and blue dashes) fit the data for the later phases without injections. The closeness of these fits suggest that approximating the whole blood volume as a single mixing chamber would give a fairly good fit too. But the exponential Test curves decay a little too rapidly compared to the model function and the data at the lowest concentrations. This systematically better fit of the model compared to the single exponential curve emphasizes that the circulation is not really instantaneously wholly mixed, and that a complete washout curve must be multi-exponential.

With respect to the physiological state of the animal, the fact that the same value for G_3 fits the data throughout the 4 hour study says that the hepatic clearance was stable over this long period of anesthesia. We can also conclude that there is no evidence for the saturation of the clearance process over the range of ICG concentrations seen here, fairly high concentrations, nearing 10 mg/L. This implies that the processes for ICG clearance are not only very effective, but must have binding constants high compared to the concentrations found here. This dye soon found use as a clinical test of liver function (Hunton, 1961), and is widely used clinically today (Krenn 2008, 2009: Kortgen, 2009). The hepatocyte's apical transporter has a very high capacity so that in the normal liver the transhepatic extraction is nearly 100% and the dye clearance can be used to estimate hepatic blood flow. The reason the extraction is so high is that there is an active ATP-supported extrusion of the dye from the hepatocyte into the bile, thus keeping the intra-hepatocyte concentration low. These features cannot be demonstrated at the low concentrations seen in Figures 8 and 9, but one would expect that the model would have to be revised to include a saturable transporter if the concentrations were a lot higher.

5. Summary: The Processes Undertaken in Pharmacokinetics

In Section 4 we covered a standard approach to the steps in a modeling analysis of data. The order of the steps depends a little on the nature of the task. In the first model we performed no verification steps, and in the second the verification was done after the fitting of the model to the data. This is clearly in the wrong order: there is no point fitting a model to the data until it has been demonstrated to be computed correctly, so in the list that follows, the verification is done as soon as the draft model is constructed. One can't argue that the verification isn't needed until the model fits the data: a mathematically incorrect model might fit the data, and after all that work the effort would be shown to be a waste if the code had an error. Our failure to precede the data fitting by a formal verification in these tow cases is based on the observations that JSim's solutions for compartmental models provides 4 digit accuracy compared to analytical solutions.

Taking a listing of the steps to a detailed level:

- Ideally, design the experimental protocol to be the best test of the model.
- Gathering supporting data, assess experimental accuracy.
- Obtain information on necessary parameters, a priori, and on possible constraints.
- Complete development of the model. List all the assumptions.

- Conduct simulations, compare the results with other methods of solution, perform verification tests, and find limiting cases for which there are analytical solutions.
- Determine how one should weight the data, for use in minimizing the sum of squares of differences between model solutions and data.
- Validate that the model is reasonable: results in good fits, residual errors are not systematic or localized.
- Comparing simulation results to experiments and/or results of other methods.
- Post-processing: analyzing the results for consistency with respect to physical and chemical and physiological expectations.
- Interpret the results scientifically. What does the model predict?
- Rethink the process. What are the weakest assumptions in the model? How might it be improved? The *model is always wrong*. Figure out new tests of it. Where might its predictions fail?

This overall process can be considered a success, if:
- Observations hitherto unexplained now fit a rational working hypothesis.
- The essence of the phenomenology has been captured. (A descriptive success only, perhaps.)
- Diagrams of relationships, defining schema of interactions, characterizing relationships quantitatively, at least descriptively and hopefully mechanistically.

6. Model Alternatives and Modifications: interative Hypothesis Revising:

When the fit is not precise, outside of the limits of expectation relative to the noise in the data, despite all the attempts, then maybe the model is just wrong. Certainly it is not nicely descriptive, let alone explanatory! Given the philosophical premise that all models are wrong, in the sense of being incomplete, or incorrect mechanistically, every failure is a stimulus to find an alternative model. A most rewarding and successful strategy is that of Platt (1964): he proposes that right from the outset one should have alternative hypotheses in mind, and that the experiment should be designed to distinguish between these hypotheses. “Strong Inference” is the title of his paper. We advocate that each hypothesis be expressed in terms of a computational model, since that means that it is described explicitly and is therefore testable. The strategy pays off because at least one of the hypotheses is proven wrong when the model fails to fit the data. Sometimes both are wrong! Regroup, rethink!

The least squares approach, minimization of the sums of squares of the differences between the data points and the model function, is a blunt tool, without specific information with respect to any misfitting. Displaying the residuals, plotting the point-by-point differences as a function of time (or in general, of the independent variable), is an excellent way to get insight into what to do next: a series of points above or below zero reveals a systematic misfitting. Comparing the time course of the deviations of the data from the model with the sensitivity functions of the various parameters could suggest that a particular parameter has not been optimized well, but this is most unlikely when the various options for optimization have been explored. It is more likely that the model lacks a feature that is needed. Back to the drawing board!

This is the usual iterative process: Hypothesize in general terms, develop the model that represents a clear precise hypothesis, if possible design the model for an alternative hypothesis,

design the distinguishing experiment while taking into account the accuracy of the data to be acquired, disprove one or both hypotheses. The next step is to improve the model and repeat the series of steps until a satisfactory level of synchrony between model and experiment is achieved. This version of the model is usually then designated the working hypothesis. Any working hypothesis is not to be regarded as "the truth", though it is useful for practical purposes. And in fact it serves as the standing target to be disproved and advance the science.

7. What to do when the compartmental representation isn't so good?

What follows is a common example that applies in biophysics, physiology and pharmacology. It is usual that drugs and substrates for metabolism and signaling molecules of molecular weight less than 1000 Daltons are partially extracted during single passage through a capillary. Since capillaries are about a 1000 microns long, but only 5 microns in diameter (as in Figure 10), there is no possibility that they are instantaneously stirred tanks with uniform concentration from end to end: there must be gradients between capillary entrance and exit for any solute that is exchanging between blood and tissue. If the extraction is less than 5%, the gradient might be ignored, but for solutes of interest to us here the steady state extractions are 30 to 90%, and so affect the estimates of the permeabilities and consumption rates. Consequently we now consider the computational differences between a stirred tank and an axially distributed capillary-tissues exchange unit.

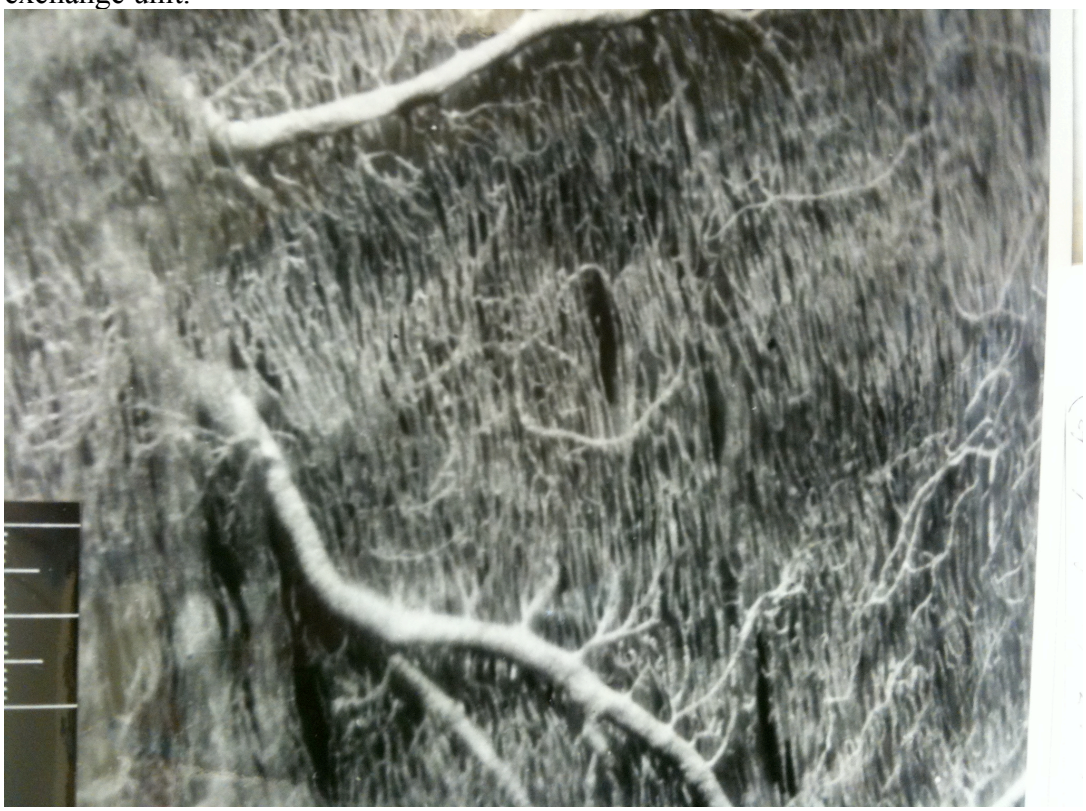

Figure 10. A venule and capillaries on the epicardium of a dog heart casted with microfil. Capillary diameters are 5.6 +/- 1.3 microns, average intercapillary distances are 17 to 19 microns, and lengths are 800 to 1000 microns. The distance between the long calibration lines are 100 microns. (Bassingthwaighte, Yipintsoi and Harvey, 1974.)

7A. Capillary-Tissue Exchange: Convention, Permeation, Reaction, and Diffusion

A two-compartment system is here modified to incorporate flow, as shown in Figure 11 (left panel), thus identifying V_1 as the vascular region, the membrane as the capillary barrier, and V_2 as the tissue. The system is considered as a homogeneously perfused organ with constant volumes and steady flow, *F,* in and out. Now, in order to put it into the context of substrate delivery and metabolism, we switch to standard physiological representation of the units, defining them per gram of organ mass. *F, PS,* and the consumption *G* have units ml g^{-1}-min^{-1}, and the volumes have units ml g^{-1}. This notation normalizes flows, substrate use, etc. to be independent of organ mass. (The model is www.physiome.org/jsim/models/webmodel/NSR/Comp2FlowExchange/, #247.)

To keep the system simple so as to focus on the blood-tissue exchange, the intratissue consumption is considered to be a first order process, as if the substrate concentration is far below the K_D for any enzymatic reaction.

In the right panel of Figure 11 is the equivalent axially distributed model that accounts for gradients in concentration along the length of the capillary. It is more general, but reduces to an exactly analogous model when the PS's are set to zero so there is no entry into the cells. Other parameters for cellular permeation and reaction are: for passage across endothelial cell luminal membrane (PSecl); endothelial cell abluminal membrane (PSeca); and parenchymal cell membrane (PSpc); G, intracellular consumption ml g^{-1}-min^{-1} or metabolism of solute by endothelial cells (Gec) or by parenchymal cells (Gpc). The Vs, ml g^{-1}, are volumes of distribution in plasma (V_{pl}), endothelial cell (V_{ec}), interstitial (V_{isf}) and parenchymal cell (V_{pc}). With the cell permeabilities, PS_{ecl}, PS_{eca}, and PS_{pc}, set to zero, then PS_g is equivalent to the compartmental PS, and V_{pl} and V_{isf} are equivalent to V_1 and V_2. In each of the four regions there is an axial dispersion coefficient, equivalent to a diffusion coefficient, setting the rate of random spreading along the length.

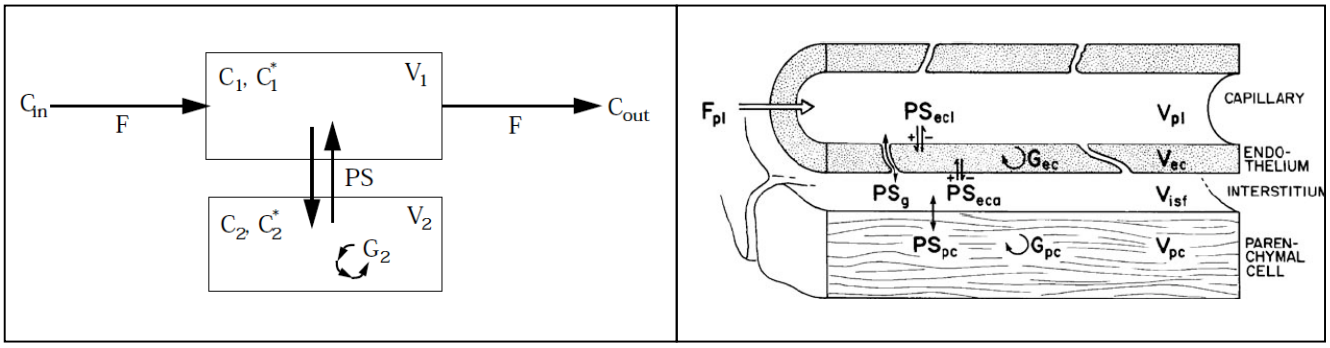

Figure 11. Compartmental versus axially distributed models for capillary-tissue exchange. Exchange between capillary plasma and interstitial fluid regions can be regarded as providing two conceptually similar but mathematical distinguishable methods of representation. *Left panel:* Two compartment stirred tank for the exchange of solute C between flowing blood and surrounding stagnant tissue. Flow F, ml g^{-1}-min^{-1}, carries in solute at concentration C_{in}, mM, and carries out a concentration C_{out}= C_p, mM. The flux from capillary to ISF (compartment 2) is limited by the conductance PS ml g^{-1}-min^{-1}, the permeability-surface area product of the membrane separating the two chambers, allowing bidirectional flux. G_2 ml g^{-1}-min^{-1} is a reaction rate for a transformation flux forming product at a rate $G_2 \cdot C_2$ mmole g^{-1}-min^{-1}. *Right panel*: Axially distributed model equivalent to the two-compartmental model when the solute does not enter the endothelial or parenchymal cells. PS_g, the conductance for permeation through the interendothelial clefts, is equivalent to the PS of the compartmental model in the left panel. (Right panel from Gorman et al. (18) with permission from the American Physiological Society.)

Chinard (1955) developed a technique to distinguish individual processes involved in blood-tissue exchange and reaction: the Multiple-Indicator Dilution (MID) technique (Figure 12) He first used it

for the purpose of estimating the volumes of distribution for sets of tracers of differing characteristics: the mean transit time volume, $V_{mtt}=F \times \bar{t}$ where $\bar{t}$ is the mean transit time through the system. He did not estimate permeabilities as his studies were on highly permeable solutes. Crone (1963) analyzed the technique, showing how it could be used to estimate *PS* from the outflow curves for a simultaneous injection into the inflow of a solute and impermeable reference intravascular tracer as shown Figure 12. The figure diagrams an experimental setup for examining the uptake of D-glucose in an isolated perfused heart as by Kuikka et al. (1986). L-glucose, the stereo-isomer, serves as an extracellular, non-metabolized reference. A more realistic diagram of a capillary–tissue exchange includes the endothelial cells and interstitial fluid (ISF), as shown in Figure 10.

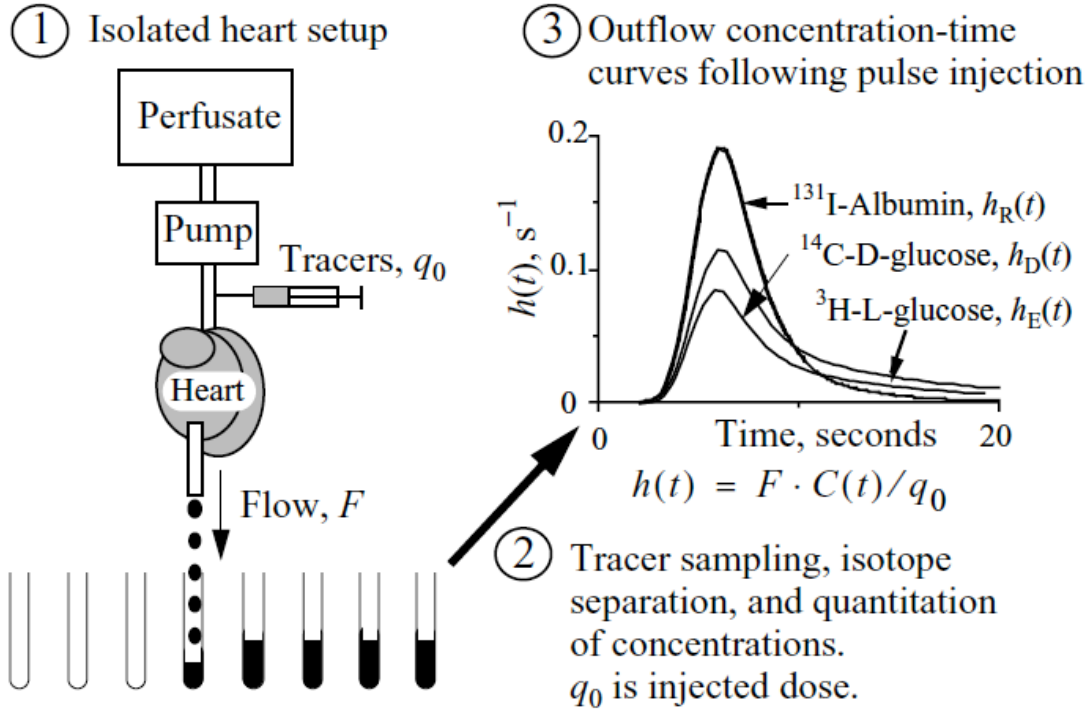

Figure 12. Schematic overview of experimental procedures underlying the application of the multiple-indicator dilution technique to the investigation of multiple substrates passing through an isolated organ without recirculation of tracer. The approach naturally extends also to their metabolites. (Figure modified from Bassingthwaighte et al 1998.)

To determine capillary permeability, the relevant reference solute is one that does not escape from the capillary blood during single transcapillary passage; for example, albumin is the relevant reference solute to determine the capillary permeability to glucose. In this situation the albumin dispersion along the vascular space may be assumed to be the same as that of the glucose; thus the shape of the albumin impulse response, $h_{alb}(t)$, accounts for the intravascular transport of all the solutes. (L-glucose, an extracellular reference tracer with the same molecular weight and diffusivity as D-glucose, is the extracellular reference for D-glucose, having the same capillary PS_g and the same interstitial volume of distribution, V_{isf}. Having simultaneous data on such reference tracers greatly reduces the degrees of freedom in estimating the parameters of interest for D-glucose.)

Model Equations for Tracer:

The two diagrams in Figure 11 look quite different, but the second can be reduced to the compartmental model, as we will show below. The essential difference is that the distributed model

accounts for concentration gradient along the capillary length. Capillaries are about 1 mm long, and are 5 microns in diameter, an aspect ratio of 200. Diffusional relaxation times thus differ by a factor of 200 between radial and axial directions. Consequently, considering the capillary as a stirred tank is unreasonable.

The stirred tank expressions account for the flow through compartment 1, the permeation, and consumption terms G_2 ml g^{-1} min^{-1} in the second compartment:

$$\frac{dC_1}{dt} = -\frac{PS}{V_1}\left(C_1 - C_2\right) - \frac{F}{V_1}\cdot(Cin - C_1).$$
$$\frac{dC_2}{dt} = +\frac{PS}{V_2}\left(C_1 - C_2\right) - \frac{G_2}{V_2}\cdot C_2. \qquad [11]$$

The use of these ODEs implies and builds into the calculations a discontinuity between the concentration of solute in the inflow and that in V_1. Because V_1 is assumed instantly mixed, there is no gradient along the capillary and the tracer entering the tank is immediately available to be washed out with the same probability as any molecule dwelling in there for a longer time. (Model #247 at www.physiome.org/jsim/models/webmodel/NSR/Comp2FlowExchange/)

Alternatively the capillary-tissue unit of Figure 10 can be reduced to two regions represented by partial differential equations (PDEs) that allow a continuous gradient along the length of the capillary between entrance and exit. Using the spatially distributed analogs for plasma, C_{pl}, or blood, and extravascular tissue, C_{isf}, instead of the lumped variables C_1 and C_2:

$$\frac{\partial C_p(x,t)}{\partial t} = \frac{F_{pl}L}{V_{pl}}\frac{\partial C_{pl}}{\partial x} + \frac{PS_g}{V_{pl}}\left(C_{pl} - C_{isf}\right) + D_{x1}\frac{\partial^2 C_1}{\partial x^2},$$
$$\frac{\partial C_{isf}(x,t)}{\partial t} = \frac{PS_g}{V_{isf}}\left(C_{pl} - C_{isf}\right) - \frac{G_{isf}}{V_{isf}}\bullet C_{isf} + D_{x2}\frac{\partial^2 C_2}{\partial x^2}, \qquad [12]$$

where C_{pl} and C_{isf} are spatially distributed functions of both x and t, not just t. The axial position is denoted by x, where $0 < x < L$, the capillary length, cm. The analogy between this model, Eqs [12], and the compartmental version in Eqs. [11] is $F_p = F$, $V_p = V_1$, $V_{isf} = V_2$, and $PS_c = PS$, the permeability-surface area of the capillary wall, but we retain the two sets of names in order to allow comparisons between the estimated parameter values. The capillary length, L, is arbitrarily set to an average value such as 0.1 cm; in the computations what is being used is the dimensionless fractional length, x/L.

PDEs require boundary conditions. At the capillary entrance, in contrast to the compartmental model there is no discontinuity in the concentration profile, but there is a requirement for matching the diffusional and convective terms so that the influx is just the convected mass, $F.C_p(x=0, t)$. The boundary conditions are written:

when (x=x.min) { $(-F_p*L/V_p)*(C_p - C_{in}) + D_p* dC_p / dx = 0$; } at inlet to capillary (13)

when (x=x.max) { $dC_p / dx = 0$; $C_{out} = C_p$;} at exit from capillary (14)

The form of the inlet condition is important when the diffusion is large, and we use it here for conceptual and practical accuracy. The outflow concentration C_{out} is set equal to the concentration just inside the exit, $C_p(x=L, t)$, the same condition described by the ODEs.

The last term in each equation is the diffusion along the length of the capillary-tissue regions; the use of an anatomically correct length then makes using observed diffusion coefficients for D_p and D_{tiss}, $cm^2\ s^{-1}$, practical and meaningful. Gross exaggeration of the diffusion coefficients can be used in the equations to turn the distributed model into a *de facto* well-mixed, compartmental model.
The flow term merits further explanation since it might appear that the sign in the first right-hand side term of Eq. [13] for the boundary condition differs from that of Eq. [12]. Consider the inflow to contain a bolus of solute: as it enters, the concentration at the capillary entrance rises. At this time, the slope of the curve of concentration versus position x, $\partial C/\partial x$, is negative as illustrated by the slope of C(x,t) for the bolus shape at t=1.5 s, at the capillary mid point, x=0.5 L. The spatial slope has always the sign opposite to the temporal derivative $\partial C/\partial t$ at the same point, thus the negative sign on the term.
Functionally, therefore Eqs. [12] are analogous to Eqs. [11]. But using the PDEs avoids the unrealistic discontinuity in the compartmental model at the entrance. Obnoxious, *unrealistic discontinuities at the entrances are the consequence of the instantaneous mixing within a compartment*. *Using the PDE allows continuity in concentrations* and concentration gradients along the capillary, and not only in concentration but also in the properties of the system such as axial gradients in transporter and enzyme densities that are evident in the liver sinusoid. For the following analysis, all parameters are assumed spatially uniform so as to minimize the difference from the compartmental models. There are many ways of representing axially distributed convecting systems, and two are shown in Figure 13. One solves PDEs using a PDE solvers (there are several choices within JSim), and here we used a Lagrangian method (Bassingthwaighte, 1974; 1992). A compartmental type of alternative is to approximate the capillary as a series of stirred tanks, each with the same volume and PS, as diagrammed in the upper part of the figure. With a large number of serial stirred tanks, the longitudinal concentration gradient is approximated increasingly accurately as the steps from one to the next are small. The intravascular transport process with serial stirred tanks is a Poisson process. In modeling, serial stirred tanks are convenient because the number of tanks, *N*tanks, can be used as a free parameter. The relative dispersion RD over the length of the tube is determined by *N*tanks such that the RD of the outflow curve, (RD equals the coefficient of variation, the standard deviation divided by the mean transit time), induced during transit is the reciprocal of the square root of *N*tanks, so that with 100 tanks the RD is 10%.

Figure 13 (upper) shows that curves for the PDE solution and for the Poisson process are essentially similar, so that the dispersion coefficient D_p sufficed to create the same dispersion as occurred with the Poisson process using 109 tanks. The choice of 109 tanks is arbitrary, large that a plot of C(*N*tanks) versus *N* would appear smooth. Because the capillary PS > 0, there is loss of solute as the bolus progresses along the capillary. The permeative loss is the same for both methods, with the result that the peak outflow concentrations are similar. Figure 13 (lower) shows the shape of the bolus as a function of position as it deforms continuously from its initial square pulse at the entrance to the capillary. The diminution in peak height is therefore due not only to the spreading but also to the loss. This loss is reflected of course in the reduction in the areas. The grey curve touching to top of each spatial profile is the theoretical curve from Crone (1963) and Renkin (1959), as in the model of Sangren and Sheppard (1954):

$$C(x) = 1 - e^{-\frac{PS_c \bullet x}{F_p \bullet L}} \qquad (15)$$

where x/L is the fractional distance along the capillary, the abscissa in the lower panel.

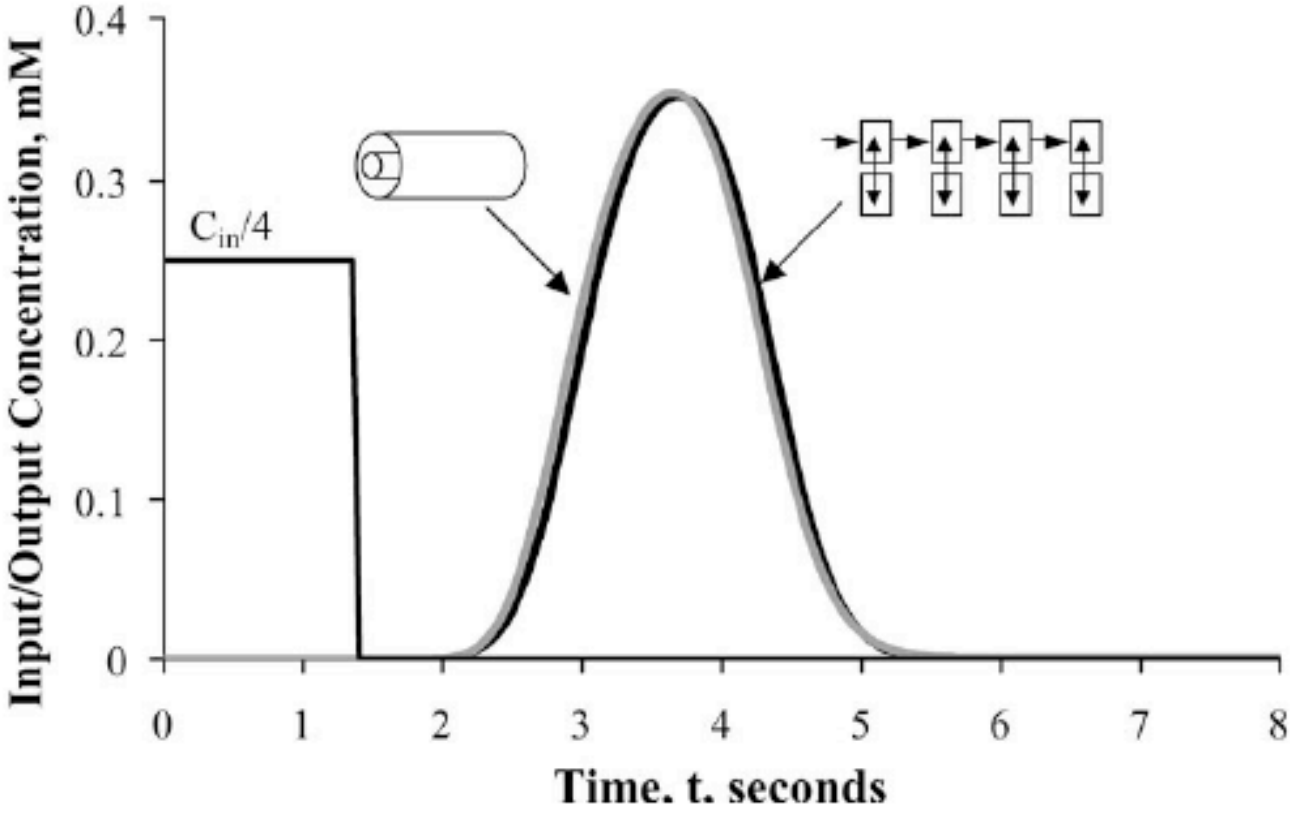
Input/Output Concentration, mM
0.4
0.3
0.2
0.1
0
$C_{in}/4$
0
1
2
3
4
5
6
7
8
Time. t. seconds

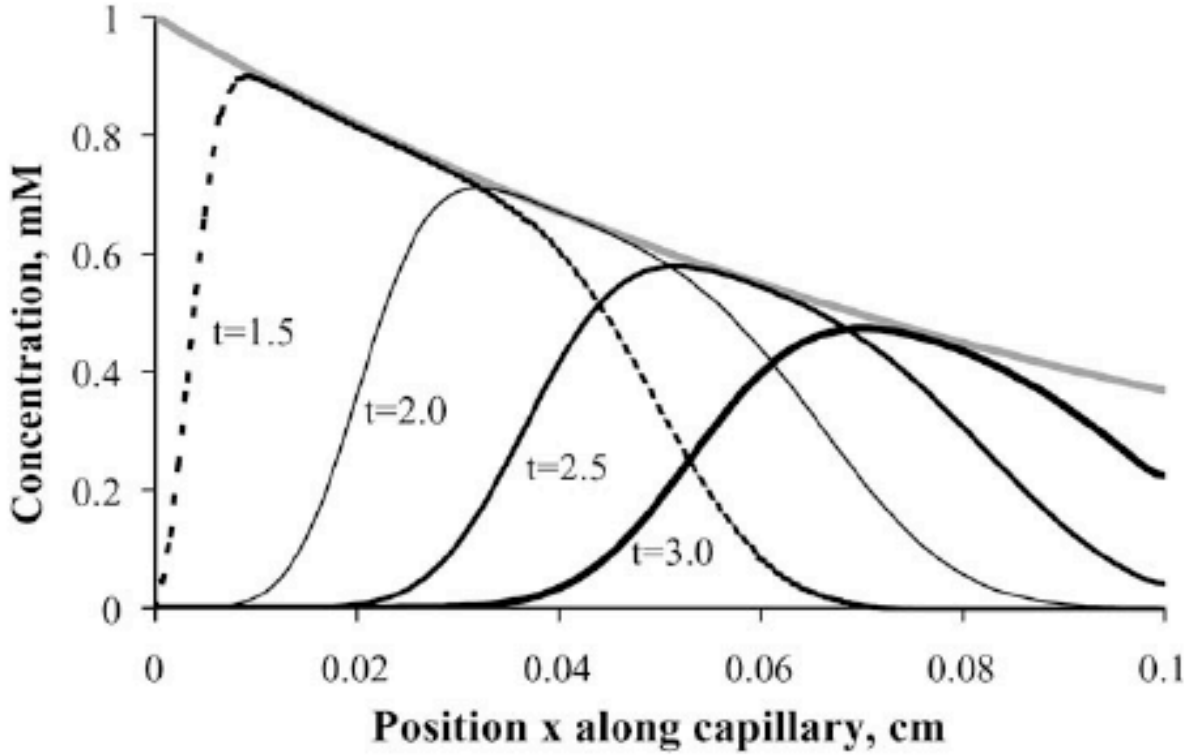
Concentration, mM
1
0.8
0.6
0.4
0.2
0
t=1.5
t=2.0
t=2.5
t=3.0
0
0.02
0.04
0.06
0.08
0.1
Position x along capillary, cm

Figure 13. Pulse responses in axially-distributed models. The input function, C_{in}, is a pulse of duration 1.4 seconds. *Upper Panel*: Outflow concentration-time curves for a partial differential equation solution using a Lagrangian sliding fluid element method and an intravascular dispersion coefficient, $D_p = 2.6 \times 10^{-5}$ cm^2 s^{-1} (gray curve), and for a serial stirred tank algorithm representing a Poisson process with 109 stirred tanks (black curve almost superimposed on the gray one). *Lower Panel*: Intracapillary spatial profiles in the distributed model (using the PDEs) at a succession of times, 1.5, 2.0, 2.5, and 3.0 seconds. The pulse slides and disperses due to the diffusion while some solute is lost from the vascular space by permeation of the capillary wall. Parameters were the same for the compartmental 109 tank Poisson model and the PDE: $F_p = 1$ ml g^{-1} min^{-1}, $PS_C = 2$ ml g^{-1} min^{-1}, and tissue volume V_{tiss} was set to 10 ml g^{-1} so that there was negligible tracer flux from tissue back into the plasma space. (The model: http://www.physiome.org/jsim/models/webmodel/NSR/Anderson_JC_2007/FIGURES/Anderson_JC_2007_fig11/index.html)

Now that we know that the multi-compartmental serial tank representation can be as good as the normal PDE representation, and that they differ basically only in the numerical method used, the question becomes. "Which of the methods produces the correct assessment of the parameters with the greatest efficiency?" The serial stirred tank model has the disadvantage that the waveforms are seriously distorted by reducing the number of stirred tanks, as is shown in Figure 14.

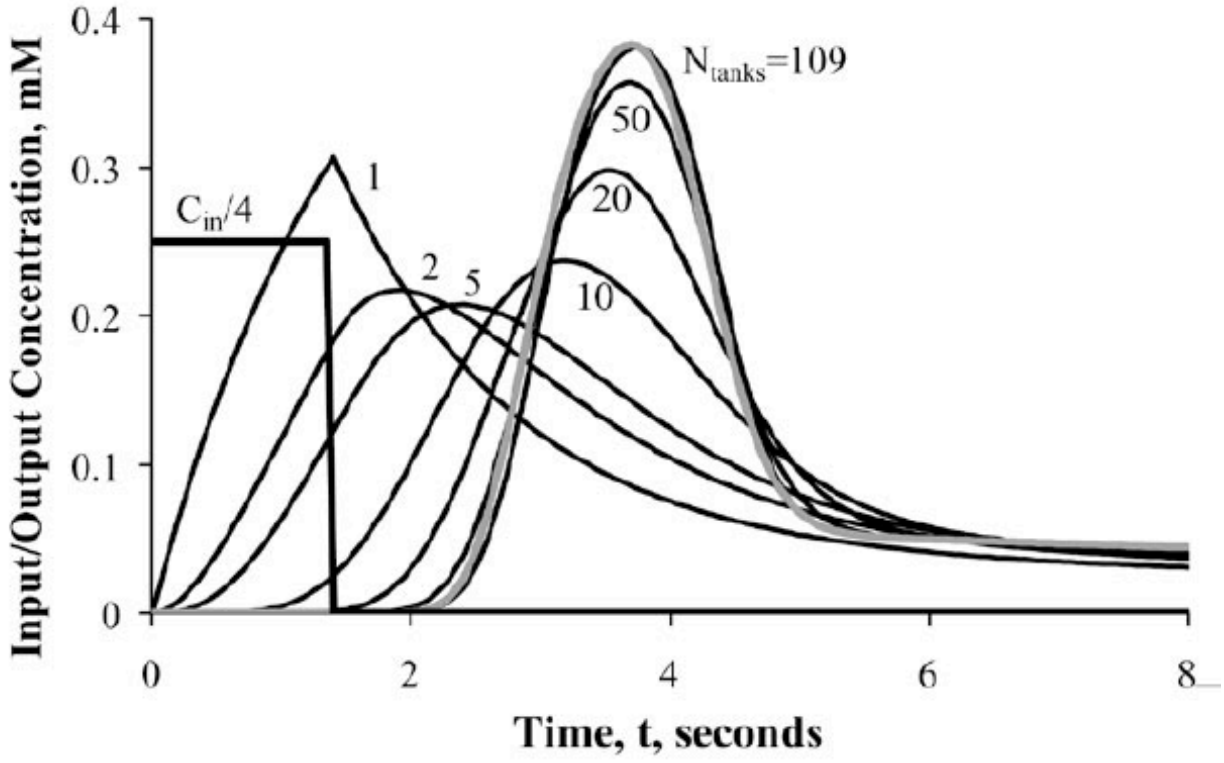

Fig 14. *Effect of reduction of Ntanks on the output C(t).* Responses of the Nth order Poisson operator with N_{tanks} varied from 109 tanks in series down to 50, 20, 10, 5, 2, and finally to a single mixing chamber, $N_{tanks} = 1$. The gray curve is the Lagrangian solution to the PDEs as in Figure 13. All of the Poisson operator outflow curves (black) have the same mean transit time, and the same parameters: $V_p = 0.05$ and $V_{tiss} = 0.15$ ml g^{-1}; $F_p = 1$ ml g^{-1} min^{-1}, $PS_C = 1$ ml g^{-1} min^{-1}. Model is #46:
http://www.physiome.org/jsim/models/webmodel/NSR/Anderson_JC_2007/FIGURES/Anderson_JC_2007_fig12/index.html)

While reducing the number of tanks in the stirred tank method has a dramatic effect on the shapes of the outflow curves, the problem is much less severe with the PDE representation, as shown in Figure 15. Solutions are shown for Ngrid = 109, 51, 21, 11, and 7 for two methods of solving PDEs, one using a robust solver TOMS731 (ACM/ TOMS) and the other using a Lagrangian sliding fluid element algorithm (Bassingthwaighte, Chan and Wang 1992).

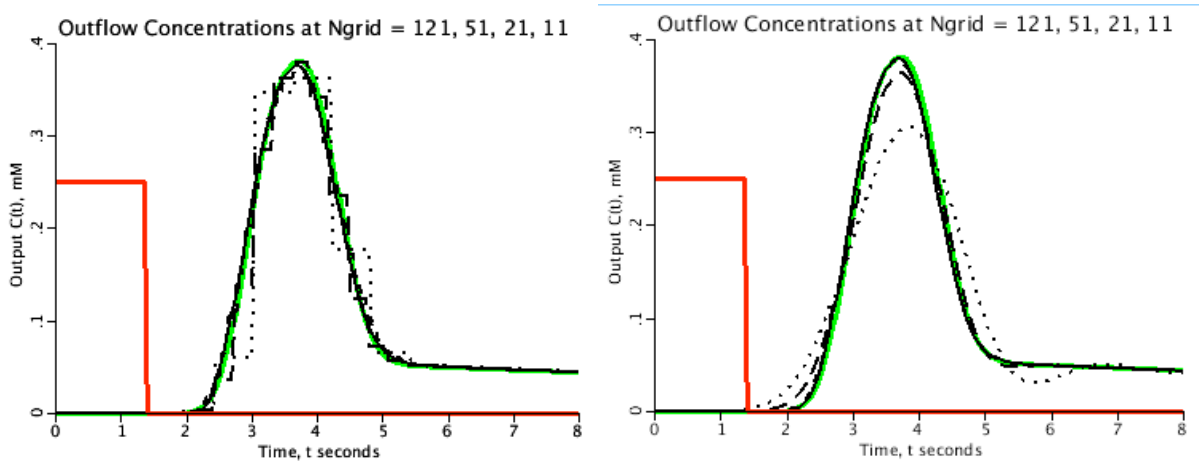

Fig. 15. *Effect of reduction of Ngrid on the output C(t) with two PDE solvers*. The green curve is the serial compartmental model with 109 tanks. The red rectangle is the input function divided by 4 in height. *Left panel*: Lagrangian sliding fluid element algorithm, LSFEA. This algorithm, while computationally fast, describes the outflow dilution curve as a series of square pulses; with a large number of segments the curves appear smooth. With fewer segments, e.g. Ngrid = 21 (long dashes) or 11 (dotted line), the steps are obvious but the approximation is reasonably good. *Right panel*: TOMS731 solver. This slow, robust solver, like most PDE solvers, broadens the solution somewhat with reduced Ngrid but with Ngrid = 11 (dotted lines) there is obvious spreading and oscillation in the solutions. (www.physiome.org Model #

Computation times for the PDE solvers are almost proportional to Ngrid the number of spatial elements chosen for the computation. LSFEA is very much faster than TOMS731, and is also faster than the serial tanks model since fewer segments are needed. The key thing is that when the number of grid points is reduced the PDE algorithms don't change shape so much as the serial compartmental models. The result is that the PDEs are more efficient for fitting the data and provide a realistic solution.

Accounting correctly for smooth intracapillary gradients is important in the analysis of indicator dilution data for low molecular weight solutes using high resolution techniques. Figure 16 is an example of modeling of the uptake of glucoses in the dog heart. The data (Kuikka, 1986) are outflow dilution curves from actively contracting blood-perfused dog hearts. Albumin is the intravascular reference data curve defining the dispersion and delay from the coronary inflow to the effluent veins for all of the tracers. The study was on D-glucose, a normal substrate, and 2-deoxy-D-glucose, an abnormal glucose that is transported into the cardiomyocyte, phosphorylated by hexokinase and then cannot be further metabolized. The model is that illustrated in Figure 11 (right panel) but without considering the negligible uptake by the endothelial cells. Parameters for the capillary wall permeation through the clefts, and for the cellular uptake are given in the legend. The quality of the data is shown by the smoothness of the

curves over time; the goodness of fit is a testimonial to the quality of the model defined through the partial differential equations.

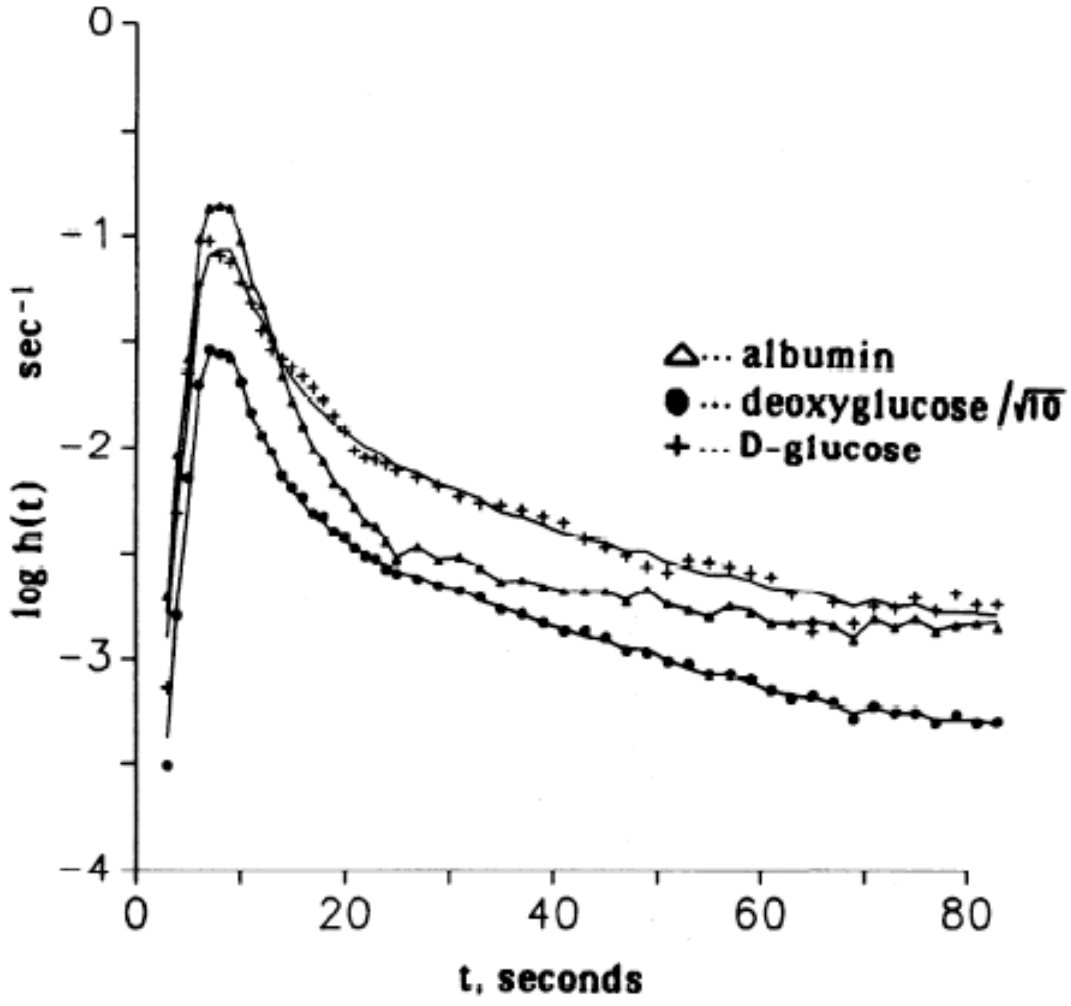

Figure 16. Outflow dilutions curves for d-glucose, 2-deoxy-D-glucose and albumin (dog expt 4048-6) fitted with the model. The deoxyglucose curve was shifted downward by half a logarithmic decade (ordinate values divided by 10") to display it separately from D-glucose curve. Parameter estimates for D- and deoxyglucose were PS_c, 0.97 and 1.0; PS_{pc} = 0.7 and 0.5; G_{pc} = 0.01 and 0.05 ml-g^{-1} min^{-1}; the volume ratio V_{isf}/V_p = 6.5 and V_{pc}/V_p = 13.3 ml/g, the same for both glucoses. Coefficients of variation were 0.19 and 0.09. (From Kuikka, 1986 with permission from the American Physiological Society.) (Model is at www.physiome.org: Search on Kuikka.)

8. COMMENTARY:

This presentation has emphasized issues important for new users of compartmental systems to contemplate. This reduced coverage neglect many important issues such as the identifiability of the models, distinguishing one option from another, the numbers and accuracy of the data

points and their timing is obtaining parameter estimates, the consequences of model verification testing, and the basic principles of numerical methods and optimization techniques. These are all covered in the more general references listed in the Introduction.

We did however carefully express the models in physiological terms, trying to emphasize recognition of the nature of the processes of exchange and reaction. Thus Equations 11 were deliberately not written in the common parlance used in compartmental modeling:

$$\frac{dC_1}{dt} = -k_1\left(C_1 - C_2\right) - k_2 \cdot (Cin - C_1).$$
$$\frac{dC_2}{dt} = +k_3\left(C_1 - C_2\right) - k_4 \cdot C_2. \qquad [15]$$

where $k_1 = PS/V_1$, $k_2 = F/V_1$, $k_3 = PS/V_2$, $k_4 = G_2/V_2$. These equations look simpler, for it appears that there are fewer parameters, namely 4, while the original equations appear to have 5: F, PS, V_1 and V_2, and G_2. But they are deceptively simple, quietly masking their true identities, behind the fact that there are really only four independent parameters in the original Eq. 11. Putting $\tau = V_1 / F$, $\gamma = V_2 / V_1$, $\delta = G_2 / F$, $\varepsilon = PS / F$, we have $k_1 = PS/V_1, = \delta / \tau$; $k_2 = F/V_1 = 1/\tau$; $k_3 = PS/V_2, = \varepsilon /(\gamma . \tau)$; and $k_4 = G_2/V_2. = \delta /(\gamma . \tau)$; this illustrates that there were only 4 parameters in the original expressions, as expected, remembering that the exponential response of a single compartmental system has just one parameter $\tau = V_1 / F$, its mean transit time. The point is that PS, G, F, and the V's have real anatomic and physiological meaning, and reminding us that when the flow is known, V_1 is the relevant unknown, and it is usually constrained by knowledge of the anatomy.

In this essay we have not emphasized the distinction between tracer and non-tracer kinetics except in the Introduction in Equations [1] to [3]. We have however considered the nonlinearity of reactions in the first application in Section 4, where the dependence of the reaction flux on the concentration is evident. If the salicylate concentration were held constant at any particular value, then for a tracer, the tracer flux would be determined entirely by the concentration of the ambient non-tracer salicylate, and the system would be reduced to a linear one with constant coefficients. Likewise, when examining tracer fluxes in a situation where mother substance is varying, this should be taken into account by computing the dual model, for mother and tracer simultaneously, a consideration all too often forgotten in the common usage of compartmental analysis. The warning is: when using tracers, measure the background concentrations of mother substance often enough to assure its constancy.

The traditional compartmental analysis therefore has its greatest strength in situations where the overall system is in steady state for all substances related to the tracer substance, for then the power of linear systems analysis applies, convolution integration and stationarity apply, and matrix inversion can be used on sets of linear ordinary differential equations. Then all is well in this best of all possible worlds.

9. REFERENCES:

ACM/TOMS. Association of Computing Machinery: Transactions on Mathematical Software. http://www.netlib.org/toms/index.html

8209. Aarons L, Hopkins K, Rowland M, Brossel S, and Thiercelin JF. Route of administration and sex differences in the pharmacokinetics of aspirin, administered as its lysine salt. Pharmaceutical Res 6: 660-666, 1989.

10615. Anderson JC and Bassingthwaighte JB. Tracers in physiological systems modeling. In: Mathematical Modeling in Nutrition and Agriculture. Proc 9th Internat Conf on Mathematical Modeling in Nutrition, Roanoke, VA, August 14-17, 2006, edited by Mark D. Hanigan JN and Casey L Marsteller. Virginia Polytechnic Institute and State University Blacksburg, VA, 2007, pp 125-159.

10007. Bassingthwaighte JB, Edwards AWT, and Wood EH. Areas of dye-dilution curves sampled simultaneously from central and peripheral sites. J Appl Physiol 17: 91-98, 1962.

10024. Bassingthwaighte JB, Ackerman FH, and Wood EH. Applications of the lagged normal density curve as a model for arterial dilution curves. Circ Res 18: 398-415, 1966.

10027. Bassingthwaighte JB. Plasma indicator dispersion in arteries of the human leg. Circ Res 19: 332-346, 1966.

10102. Bassingthwaighte JB, Yipintsoi T, and Harvey RB. Microvasculature of the dog left ventricular myocardium. Microvasc Res 7: 229-249, 1974.

10108. Bassingthwaighte JB. A concurrent flow model for extraction during transcapillary passage. Circ Res 35: 483-503, 1974.

10242. Bassingthwaighte JB, Chinard FP, Crone C, Goresky CA, Lassen NA, Reneman RS, and Zierler KL. Terminology for mass transport and exchange. Am J Physiol Heart Circ Physiol 250: H539-H545, 1986.

10312. Bassingthwaighte JB, Wang CY, and Chan IS. Blood-tissue exchange via transport and transformation by endothelial cells. Circ Res 65: 997-1020, 1989.

10371. Bassingthwaighte JB, Chan IS, and Wang CY. Computationally efficient algorithms for capillary convection-permeation-diffusion models for blood-tissue exchange. Ann Biomed Eng 20: 687-725, 1992.

10476. Bassingthwaighte JB, Goresky CA, and Linehan JH. Ch. 1 Modeling in the analysis of the processes of uptake and metabolism in the whole organ. In: Whole organ approaches to cellular metabolism, edited by Bassingthwaighte JB, Goresky CA, and Linehan JH. New York: Springer Verlag, 1998, pp 3-27.

10573. Bassingthwaighte JB and Vinnakota KC. The computational integrated myocyte. A view into the virtual heart. In: Modeling in Cardiovascular Systems. Ann. New York Acad. Sci. 1015:,

edited by S. Sideman and R. Beyar. 2004, p. 391-404.

10596. Bassingthwaighte JB, Raymond GR, Ploger JD, Schwartz LM, and Bukowski TR. GENTEX, a general multiscale model for [italic] in vivo [plain] tissue exchanges and intraorgan metabolism. Phil Trans Roy Soc A: Mathematical, Physical and Engineering Sciences 364(1843): 1423-1442, 2006.

7311. Beard DA, Liang S, and Qian H. Energy balance for analysis of complex metabolic networks. Biophys J 83: 79-86, 2002.

8208. Benedek IH, Joshi AS, Pieniazek JH, King S-YP, and Kornhauser DM. Variability in the pharmacokinetics and pharmacodynamics of low dose aspirin in healthy male volunteers. J Clin Pharmacol 35: 1181-1186, 1995.

38. Berman M. The formulation and testing of models. Ann NY Acad Sci 108: 182-194, 1963.

387. Chan IS, Goldstein AA, and Bassingthwaighte JB. SENSOP: A derivative-free solver for non-linear least squares with sensitivity scaling. Ann Biomed Eng 21: 621-631, 1993.

87. Chinard FP, Vosburgh GJ, and Enns T. Transcapillary exchange of water and of other substances in certain organs of the dog. Am J Physiol 183: 221-234, 1955.

Cobelli C, Foster D, and Toffolo G. Tracer Kinetics in Biomedical research. From data to model. Kluwer Academic/Plenum Publishers, New York, 2000.

10632. Chizeck HJ, Butterworth E, and Bassingthwaighte JB. Error detection and unit conversion. Automated unit balancing in modeling interface systems. IEEE Eng Med Biol 28(3): 50-58, 2009.

99. Crone C. The permeability of capillaries in various organs as determined by the use of the indicator diffusion method. Acta Physiol Scand 58: 292-305, 1963.

10580. Dash RK and Bassingthwaighte JB. Blood HbO2 and HbCO2 dissociation curves at varied O2, CO2, pH, 2,3-DPG and temperature levels. Ann Biomed Eng 32: 1676-1693, 2004.

10598. Dash RK, Li Z, and Bassingthwaighte JB. Simultaneous blood-tissue exchange of oxygen, carbon dioxide, bicarbonate, and hydrogen ion. Ann Biomed Eng 34: 2006.

807. Dennis JE and Schnabel RB. Numerical methods for unconstrained optimization and nonlinear equation. N. Y.: Prentice-Hall, 1983.

10012. Edwards AWT, Isaacson J, Sutterer WF, Bassingthwaighte JB, and Wood EH. Indocyanine green densitometry in flowing blood compensated for background dye. J Appl Physiol 18: 1294-1304, 1963.

Fox IJ, Brooker LGS, Heseltine, DW, Essex, HE, and Wood, EH. A tricarbocyanine dye for continuous recording of dilution curves in whole blood independent of variations in blood oxygen saturation. Proc. Staff Mtg Mayo Clin. 32: 478, 1957.

10234. Gorman MW, Bassingthwaighte JB, Olsson RA, and Sparks HV. Endothelial cell uptake of adenosine in canine skeletal muscle. Am J Physiol Heart Circ Physiol 250: H482-H489, 1986.

8034. Hucka ML, Finney A, Sauro HM, Bolouri H, Doyle JC, and Kitano H. The system biology markup language (SBML) a medium for representation and exchange of biochemical network models. Bioinformatics 19(4): 524-531, 2003.

Hunton, Donald B, Bollman, Jesse L, and Hoffman, Harry N. The plasma removal of indocyanine green and sulfobromophthalein: Effect of dosage and blocking agents. J. Clin Invest. 30(9): 1648-1655, 1961 (PNCID PMC290858)

7905. International Commission on Radiological Protection. Basic Anatomical and Physiological Data for Use in Radiological Protection: Reference Values. New York: Elsevier Science, 2003, 320 pp.

298. Jacquez JA. Compartmental analysis in biology and medicine. Kinetics of distribution of tracer-labeled materials. Amsterdam: Elsevier Publishing Co., 1972, pp. 237.

8074. Jacquez JA. Compartmental analysis in biology and medicine. 3rd ed. Ann Arbor, MI: BioMedware, 1996, 514 pp.

5186. Kassab GS, Rider CA, Tang NJ, and Fung Y-CB. Morphometry of pig coronary arterial trees. Am J Physiol Heart Circ Physiol 265: H350-H365, 1993.

17033. King RB and Butterworth E. XSIM -- An X-window based simulation interface. In: National Simulation Resource Website. Seattle, WA: http://www.physiome.org/software/xsim/, 1998.

10054. Knopp TJ, Anderson DU, and Bassingthwaighte JB. SIMCON--Simulation control to optimize man-machine interaction. Simulation 14: 81-86, 1970.

8211. Kortgen A, Paxian M, Werth M, Recknagel P, Rauschfusz F, Lupp A, Krenn C, Muller D, Claus RA, Reinhart K, Settmacher U, and Bauer M. Prospective assessment of hepatic function and mechanisms of dysfunction in the critically ill. Shock 32(4): 358-365, 2009.

8212. Krenn CG, Krafft P, Schaefer B, Pokorny H, Schneider B, Pinsky MR, and Steltzer H. Effects of positive end-expiratory pressure on hemodynamics and indocyanine green kinetics in patients after orthotopic liver transplantation. Crit Care Med 28: 1760-1765, 2000.

8213. Krenn C. G., Pokorny H, Hoerauf K, Stark J, Roth E, Steltzer H, and Druml W. Non-isotopic tyrosine kinetics using an alanyl-tyrosine dipeptide to assess graft function in liver transplant recipients - a pilot study.. Wien Klin Wochenschr 120/1-2: 19-24, 2008.

320. Krogh A. The number and distribution of capillaries in muscles with calculations of the oxygen pressure head necessary for supplying the tissue. J Physiol (Lond) 52: 409-415, 1919.

10233. Kuikka J, Levin M, and Bassingthwaighte JB. Multiple tracer dilution estimates of D- and 2-deoxy-D-glucose uptake by the heart. Am J Physiol Heart Circ Physiol 250: H29-H42,

1986.

10458. Li Z, Yipintsoi T, and Bassingthwaighte JB. Nonlinear model for capillary-tissue oxygen transport and metabolism. Ann Biomed Eng 25: 604-619, 1997.

3966. Platt JR. Strong inference. Science 146: 347-353, 1964.

10457. Poulain CA, Finlayson BA, and Bassingthwaighte JB. Efficient numerical methods for nonlinear facilitated transport and exchange in a blood-tissue exchange unit. Ann Biomed Eng 25: 547-564, 1997.

8210. Prescott LF, Balali-Mood M, Critchley JAJH, Johnstone AF, and Proudfoot AT. Diuresis or urinary alkalinisation for salicylate poisoning? Br Med J 285: 1383-1386, 1982.

10566. Raymond GM, Butterworth E, and Bassingthwaighte JB. JSIM: Free software package for teaching phyiological modeling and research. Exper Biol 2003 280.5, p102, 2003. (www.physiome.org/jsim)

479. Renkin EM. Transport of potassium-42 from blood to tissue in isolated mammalian skeletal muscles. Am J Physiol 197: 1205-1210, 1959.

512. Sangren WC and Sheppard CW. A mathematical derivation of the exchange of a labeled substance between a liquid flowing in a vessel and an external compartment. Bull Math Biophys 15: 387-394, 1953.

Sauro, H. M. and Fell, D. A. (1991). SCAMP: A metabolic simulator and control analysis program. Mathl. Comput. Modelling, 15:15–28.

Sauro, H. M., Hucka, M., Finney, A., and Bolouri, H. (2001). The Systems Biology Workbench concept demonstrator: Design and implementation. Available via the World Wide Web at http://www.cds.caltech.edu/erato/sbw/docs/detailed-design/.

10529. Schwartz LM, Bukowski TR, Ploger JD, and Bassingthwaighte JB. Endothelial adenosine transporter characterization in perfused guinea pig hearts. Am J Physiol Heart Circ Physiol 279: H1502-H1511, 2000.

Urquhart J and Li CC. The dynamics of adrenocortical secretion. Am J Physiol 214: 73-85, 1968

7931. Vinnakota K, Kemp ML, and Kushmerick MJ. Dynamics of muscle glycogenolysis modeled with pH time-course computation and pH dependent reaction equilibria and enzyme kinetics. Biophys J doi:10.1529/biophys.105.073296: 1-64, 2007.

10572. Vinnakota K and Bassingthwaighte JB. Myocardial density and composition: A basis for calculating intracellular metabolite concentrations. Am J Physiol Heart Circ Physiol 286: H1742-H1749, 2004.

10084. Yipintsoi T, Scanlon PD, and Bassingthwaighte JB. Density and water content of dog ventricular myocardium. Proc Soc Exp Biol Med 141: 1032-1035, 1972.

658. Zierler KL. A critique of compartmental analysis. Annu Rev Biophys Bioeng 10: 531-562, 1981.

NEEDS:

MODEL REFERENCES FOR FIGS 15 AND 16